

School on the Physics of Equatorial Atmosphere
(24 September - 5 October 2001)

Waves in the Tropical Middle Atmosphere

R. Garcia
(National Center for Atmospheric Research, Boulder)

Waves in the Tropical Middle Atmosphere

1. Introduction

- Why tropical dynamics is different
- An example: Zonal wind evolution in the stratosphere
- Coupling between waves and the zonal mean state in the Tropics

2. Waves in the Tropics: Theory

- Tropical vs. Extratropical Waves
- The Equatorial β -plane
- The Kelvin wave: Equatorial trapping
- Other equatorial waves
- Small-scale gravity waves

3. Waves in the Tropics: Observations

Extratropical vs. Tropical Dynamics

1. Zonal Mean Equations

$$\begin{aligned}
 \bar{u}_t + \bar{v}^* \bar{u}_y + \bar{w}^* \bar{u}_z - f \bar{v}^* &= \mathcal{F} && \text{zonal momentum} \\
 \bar{v}_y^* + \rho^{-1} (\rho \bar{w}^*)_z &= 0 && \text{continuity} \\
 f \bar{u} &= -\bar{\phi}_y && \text{meridional momentum} \\
 \bar{\phi}_{zt} + \bar{v}^* \bar{\phi}_{zy} + \bar{w}^* S &= -\alpha \bar{\phi}_z && \text{thermodynamics}
 \end{aligned}$$

2. Quasi-steady motions outside Tropics

- momentum balance $-f \bar{v}^* \simeq \mathcal{F}$
- this implies (\bar{v}^*, \bar{w}^*) are determined by \mathcal{F}
- in turn this determines $\bar{\phi}$ via $\bar{w}^* S = -\alpha \bar{\phi}_z$
- and \bar{u} via $f \bar{u} = -\bar{\phi}_y$

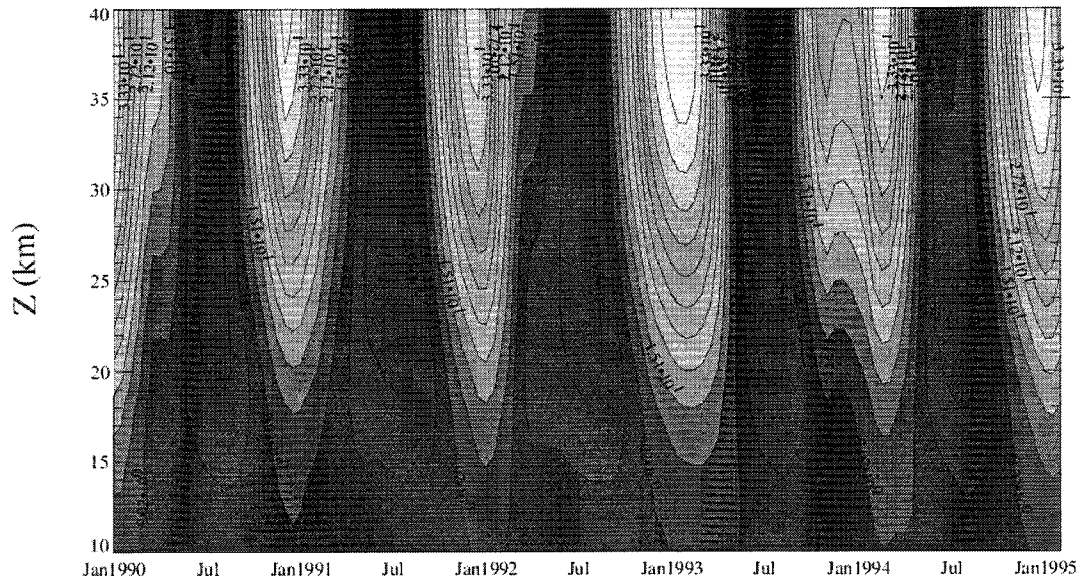
3. Low-frequency motions in Tropics ($f \rightarrow \beta y$)

- f does not dominate, so all terms in the zonal momentum equation are potentially important

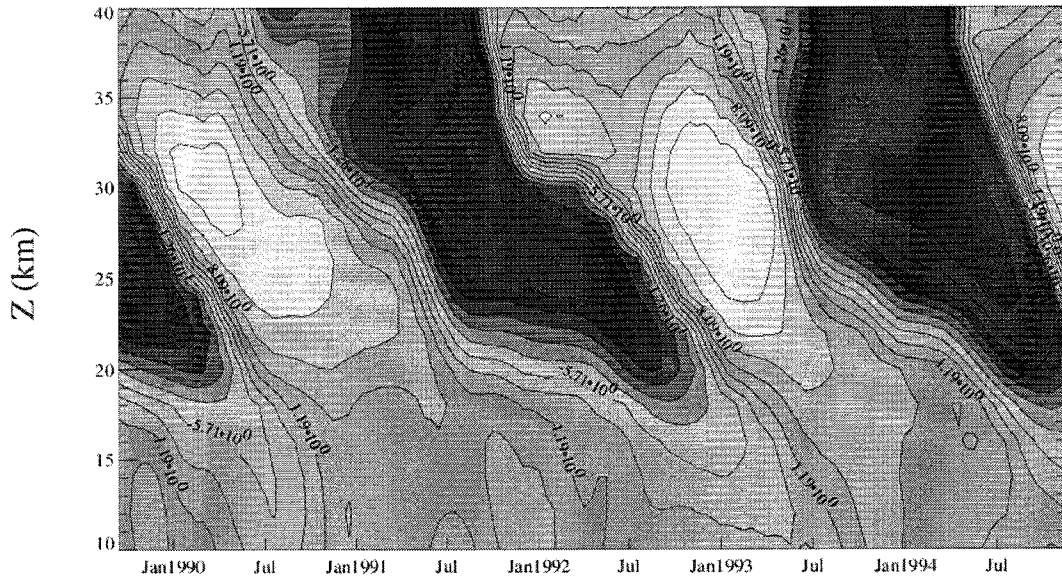
$$\bar{u}_t + \bar{v}^* \bar{u}_y + \bar{w}^* \bar{u}_z - \beta y \bar{v}^* = \mathcal{F}$$

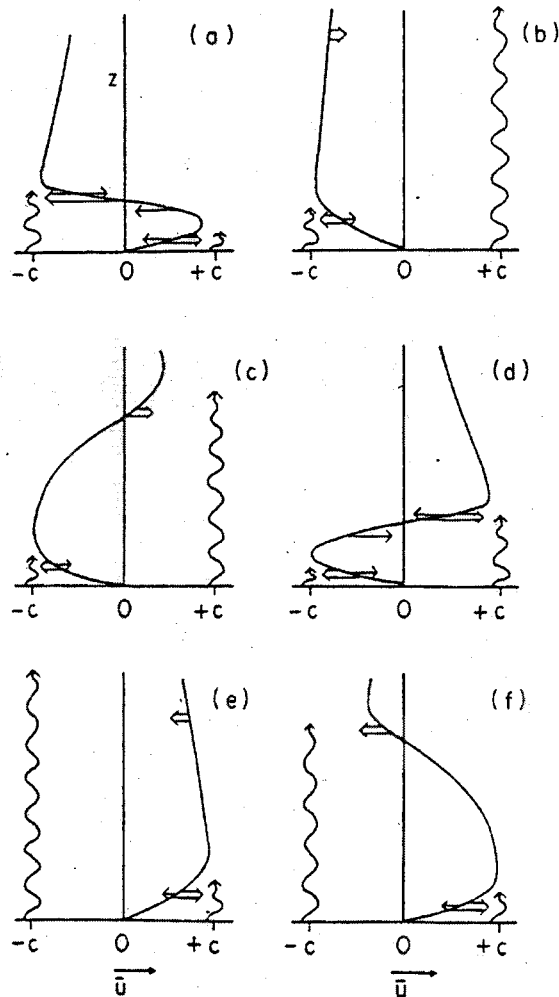
- \mathcal{F} can give rise to long-period oscillations in \bar{u} (SAO, QBO) instead of a quasi-steady-state
- \bar{u} remains in geostrophic balance $\beta y \bar{u} = -\bar{\phi}_y$

U (60 N) (m/s)



U (Eq) (m/s)





Schematic representation of the evolution of the mean flow in Plumb's analog of the QBO. Six stages of a complete cycle are shown. Double arrows show wave-driven accelerations and single arrows show viscously driven accelerations. Wavy lines indicate relative penetration of easterly and westerly waves. See text for details. [After Plumb (1984).]

Extratropical Rossby Waves vs. Equatorial Waves

1. Extratropical large-scale waves are quasi-geostrophic and quasi-non-divergent
 - their restoring force is due to the variation of f with latitude
 - gravity (which acts through the divergence field) is not of first order importance
 - the motion is described by the quasi-geostrophic vorticity equation
 - the waves described by this equation are extratropical Rossby waves
2. Tropical large-scale waves respond both to variations in f and to gravity (buoyancy) forces
 - divergence is important for tropical waves
 - tropical waves are equatorially trapped, the trapping being most effective at low frequencies

The Equatorial beta-plane

- The Equatorial β -plane approximation for latitudes θ close to the equator is $a \sin \theta \simeq a\theta = y$, which yields the following linearized system of equations:

$$\begin{aligned} \frac{\partial u'}{\partial t} - \beta y v' &= -\phi'_x \\ \frac{\partial v'}{\partial t} + \beta y u' &= -\phi'_y \\ \frac{\partial u'}{\partial x} + \frac{1}{\rho} \frac{\partial(\rho w')}{\partial z} &= 0 \\ \frac{\partial \phi'_z}{\partial t} + w' N^2 &= 0 \end{aligned}$$

- Assuming a solution of the form,

$$(u', v', w', \phi') = (\hat{u}, \hat{v}, \hat{w}, \hat{\phi}) \cdot \exp(z/2H) \cdot \exp i(kx + mz - \omega t)$$

yields the Equatorial β -plane system:

$$\begin{aligned} -i\omega \hat{u} - \beta y \hat{v} &= -ik \hat{\phi} \\ -i\omega \hat{v} + \beta y \hat{u} &= -\hat{\phi}_y \\ ik \hat{u} + \hat{v}_y + im \hat{w} &= 0 \\ -i\omega \hat{\phi}'_z + \hat{w} N^2 &= 0 \end{aligned}$$

where it has also been assumed that $m^2 \gg (1/4H)^2$ (Boussinesq approximation)

The Equatorial Kelvin Wave

- A special case, wherein $\hat{v} = 0$
- The equations on the equatorial beta-plane are then:

$$\begin{aligned} -i\omega\hat{u} &= -ik\hat{\phi} \\ \beta y\hat{u} &= -\hat{\phi}_y \\ ik\hat{u} + im\hat{w} &= 0 \\ -i\omega\hat{\phi}'_z + \hat{w}N^2 &= 0 \end{aligned}$$

- Note that $\hat{\phi}_x = ik\hat{\phi}$ is balanced by a zonal acceleration (as in a pure gravity wave) while $\hat{\phi}_y$ is balanced by the Coriolis force (as in Rossby waves)
- These equations have the simple solution

$$\hat{\phi} \propto \exp\left[-\frac{y^2}{2L^2}\right]$$

which follows upon elimination of \hat{u} , \hat{w} , and where:

$$L^2 = \frac{\omega}{\beta k}$$

(which implies $\omega > 0$)

- The complete solution is:

$$\phi' \propto \exp\left[-\frac{y^2}{2L^2}\right] \cdot \exp(z/2H) \cdot \exp i(kx + mz - \omega t)$$

- The dispersion relation is:

$$\omega = -kN/m, \quad m < 0$$

where the negative root is chosen to insure that the vertical group velocity is upward:

$$c_{gz} = \frac{\partial \omega}{\partial m} = \frac{kN}{m^2}$$

and where $m < 0$ so that $\omega > 0$ and $L^2 = \omega/\beta k > 0$

- Note this also implies that L^2 can be written as

$$L^2 = \frac{N}{\beta|m|}$$

- Other wave fields follow directly from the β -plane equations:

$$\hat{u} \propto \left(\frac{ik}{\omega}\right) \hat{\phi}$$

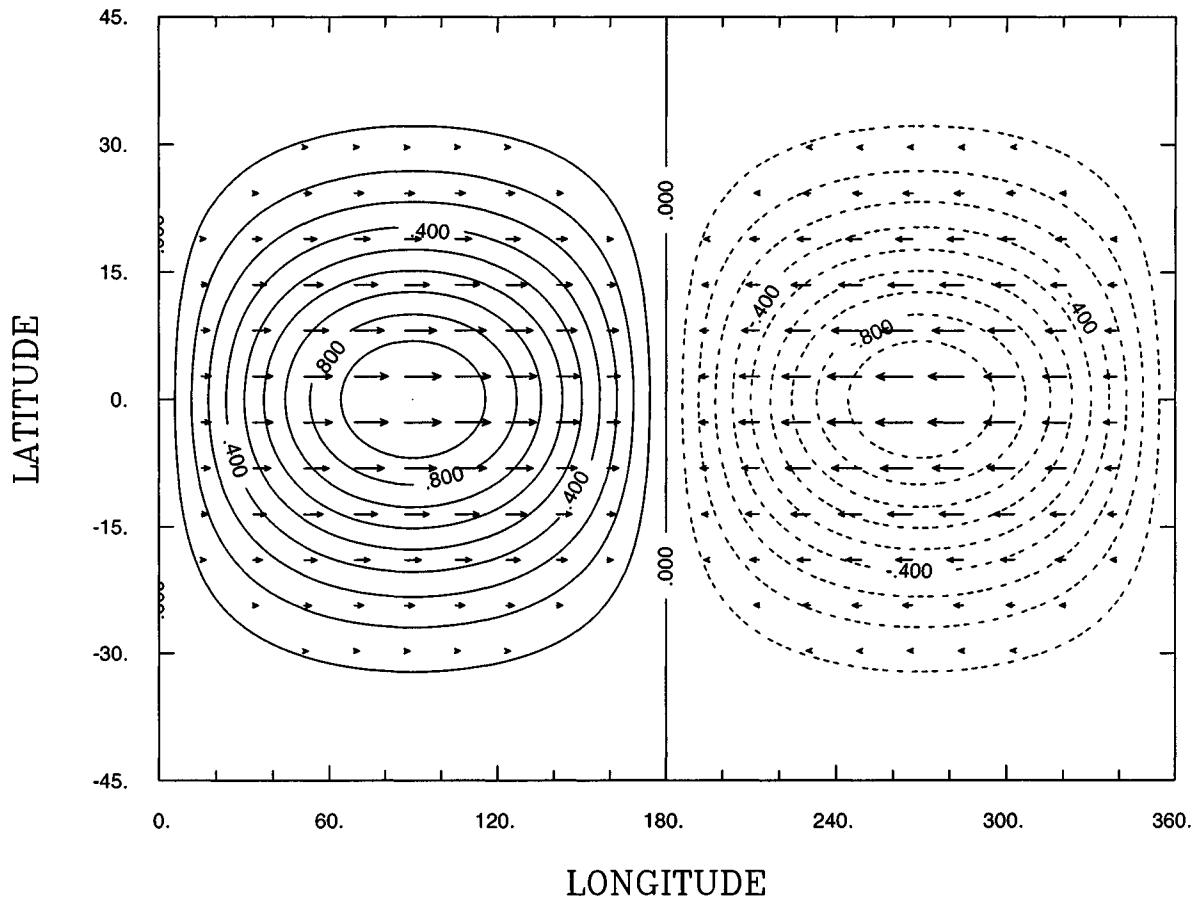
$$\hat{w} \propto -\left(\frac{\omega}{N^2}\right) \left(m - \frac{i}{2H}\right) \hat{\phi}$$

so that

$$u' \propto \left(\frac{ik}{\omega}\right) \exp\left[-\frac{y^2}{2L^2}\right] \cdot \exp(z/2H) \cdot \exp i(kx + mz - \omega t)$$

$$w' \propto -\left(\frac{\omega}{N^2}\right) \left(m - \frac{i}{2H}\right) \cdot \exp(z/2H) \cdot \exp i(kx + mz - \omega t)$$

Phi $k = 1$, $Lz = 20$. km, $n = -1$, $f = 0.14$ cpd



CONTOUR FROM -1.0000 TO 1.0000 CONTOUR INTERVAL OF 0.10000 PT(3,3)= 0.16498E-02

0.157E-01
→
MAXIMUM VECTOR

Other Equatorial Waves

- Are general solutions of the equatorial β -plane equations ($v' \neq 0$)
- Again assuming solutions of the form
 $(u', v', w', \phi') = (\hat{u}, \hat{v}, \hat{w}, \hat{\phi}) \cdot \exp(z/2H) \cdot \exp i(kx + mz - \omega t)$

the general β -plane equations can be combined to give:

$$\left[\frac{d^2}{dy^2} + \left(\frac{m^2 \omega^2}{N^2} - k^2 - \frac{\beta k}{\omega} \right) - \frac{\beta^2 m^2}{N^2} y^2 \right] \hat{v} = 0$$

- This is formally identical to the “quantum harmonic oscillator” equation,
- It has solutions \hat{v} of the form

$$\hat{v} = \hat{v}_o \exp\left(-\frac{y^2}{2L^2}\right) H_n(y/L) \quad L^2 = \frac{N}{\beta|m|}$$

$$v' = \hat{v}_o \exp\left(-\frac{y^2}{2L^2}\right) H_n(y/L) \cdot \exp(z/2H) \cdot \exp i(kx + mz - \omega t)$$

where H_n are Hermite polynomials, whose index n must satisfy:

$$\frac{m^2 \omega^2}{N^2} - k^2 - \frac{\beta k}{\omega} = (2n + 1) \frac{\beta|m|}{N}$$

which acts as the dispersion relation for the waves

- Using the recursion relations for Hermite polynomials:

$$H_{n+1}(y/L) = 2(y/L)H_n(y/L) - 2nH_{n-1}(y/L)$$

$$\frac{d}{dy}H_n(y/L) = (2n/L)H_{n-1}(y/L)$$

solutions for other fields follow from the β -plane equations:

$$\hat{u} = i\hat{v}_o(\beta m N)^{1/2} \left[\frac{0.5H_{n+1}}{|m|\omega - Nk} + \frac{nH_{n-1}}{|m|\omega + Nk} \right] \cdot \exp\left(-\frac{y^2}{2L^2}\right)$$

$$\hat{\phi} = i\hat{v}_o \left(\frac{\beta N^3}{m}\right)^{1/2} \left[\frac{0.5H_{n+1}}{|m|\omega - Nk} - \frac{nH_{n-1}}{|m|\omega + Nk} \right] \cdot \exp\left(-\frac{y^2}{2L^2}\right)$$

- The solutions can be categorized under several types, according to their dispersion relationship:
 - eastward-propagating and westward-propagating gravity waves
 - westward-propagating equatorial Rossby waves
 - Rossby-gravity waves (these resemble Rossby waves for $\omega < 0$ and Kelvin waves for $\omega > 0$)
- See Gill (1982), Andrews et al (1987), and Matsuno (1966), for detailed discussions

Waves with $n > 0$

- they obey the general dispersion relation:

$$\frac{m^2\omega^2}{N^2} - k^2 - \frac{\beta k}{\omega} = (2n + 1)\frac{\beta|m|}{N}$$

which has two solution branches (Gill, 1982)

- an upper (high-frequency) branch for which

$$\omega \simeq -\frac{N}{m} \left[k^2 + (2n + 1)\frac{\beta|m|}{N} \right]^{1/2}$$

which corresponds to eastward-propagating inertia-gravity waves ($\omega > 0$) when $m < 0$, and to westward-propagating waves ($\omega < 0$) when $m > 0$

- a lower (low-frequency) branch for which

$$\omega = \frac{-\beta k}{\left[k^2 + (2n + 1)\frac{\beta|m|}{N} \right]}$$

which corresponds to equatorial Rossby waves

- Large- k limits:

$$\omega \rightarrow \pm \frac{kN}{|m|}$$

for the inertia-gravity waves, and

$$\omega \rightarrow -\beta/k$$

for the Rossby waves

Waves with $n = 0$

- their dispersion relation is:

$$\frac{|m|\omega}{N} - k = \frac{\beta N}{\omega}$$

which has solutions

$$\omega = \frac{kN}{2|m|} \cdot \left[1 \pm \left(1 + \frac{4\beta|m|}{k^2N} \right)^{1/2} \right]$$

- these waves are known as Rossby-gravity waves
- they behave like inertia-gravity waves for $\omega > 0$ (the positive root above), and as Rossby waves for $\omega < 0$ (the negative root)
- The large- k limit for the eastward $n = 0$ wave is

$$\omega \rightarrow \frac{kN}{|m|}$$

while, for the eastward $n = 0$ wave,

$$\omega \rightarrow -\beta/k$$

- These are the same limits as for the $n > 0$ eastward-propagating inertia-gravity wave and the $n > 0$ Rossby wave, respectively
- At large k , eastward-propagating waves of $n = 0$ behave like inertia-gravity waves, while westward-propagating waves behave like Rossby waves

Note also that:

- Kelvin waves behave like eastward-propagating gravity waves
- Previous results can be generalized to case with a uniform background wind U ; then $c \rightarrow \hat{c} = c - U$
- Thus, for gravity waves,

$$\hat{\omega} = k\hat{c} = k(c - U) = \pm \frac{kN}{|m|}$$

- It follows that

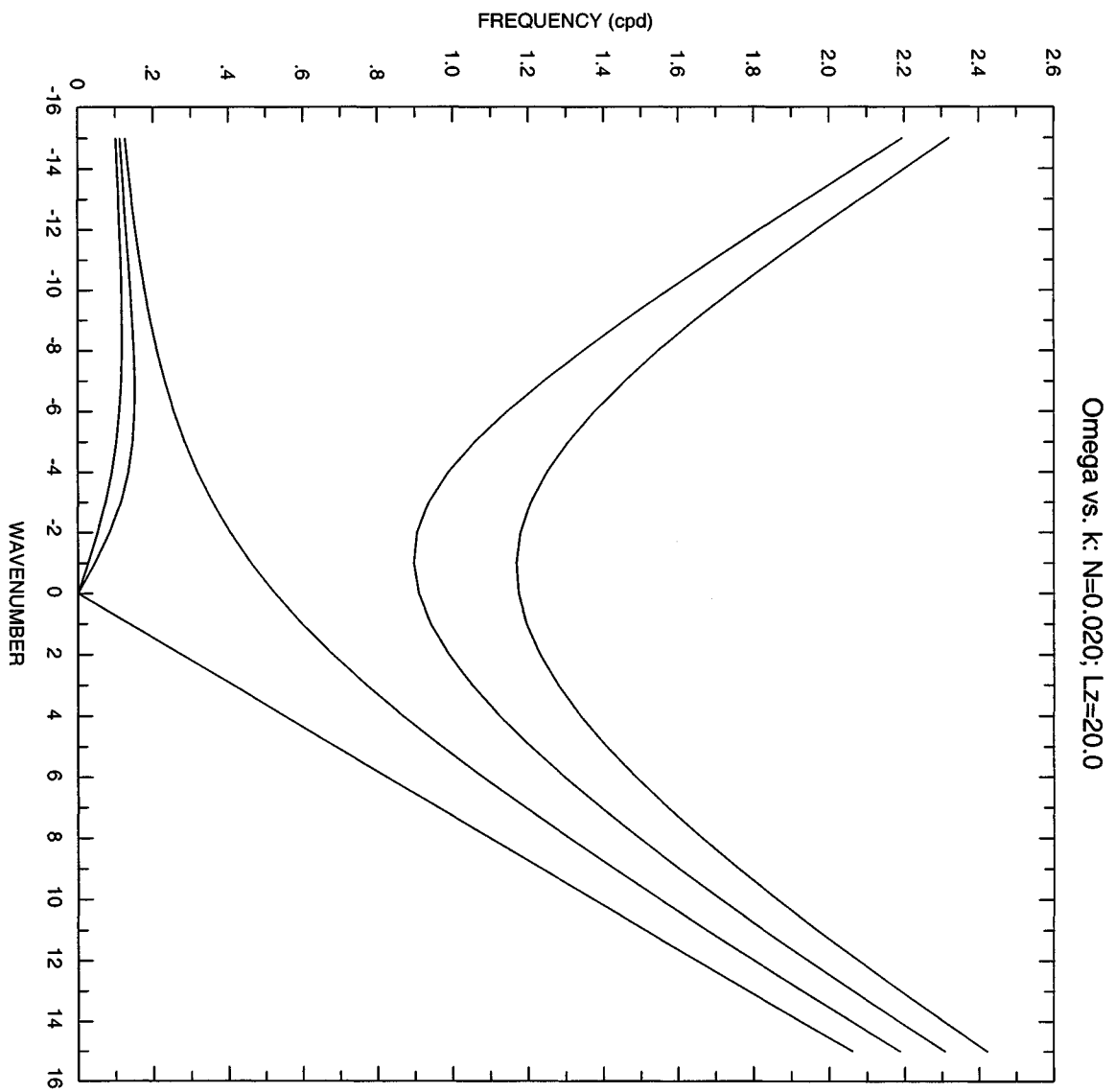
$$m = \pm \frac{N}{k|\hat{c}|}$$

so that

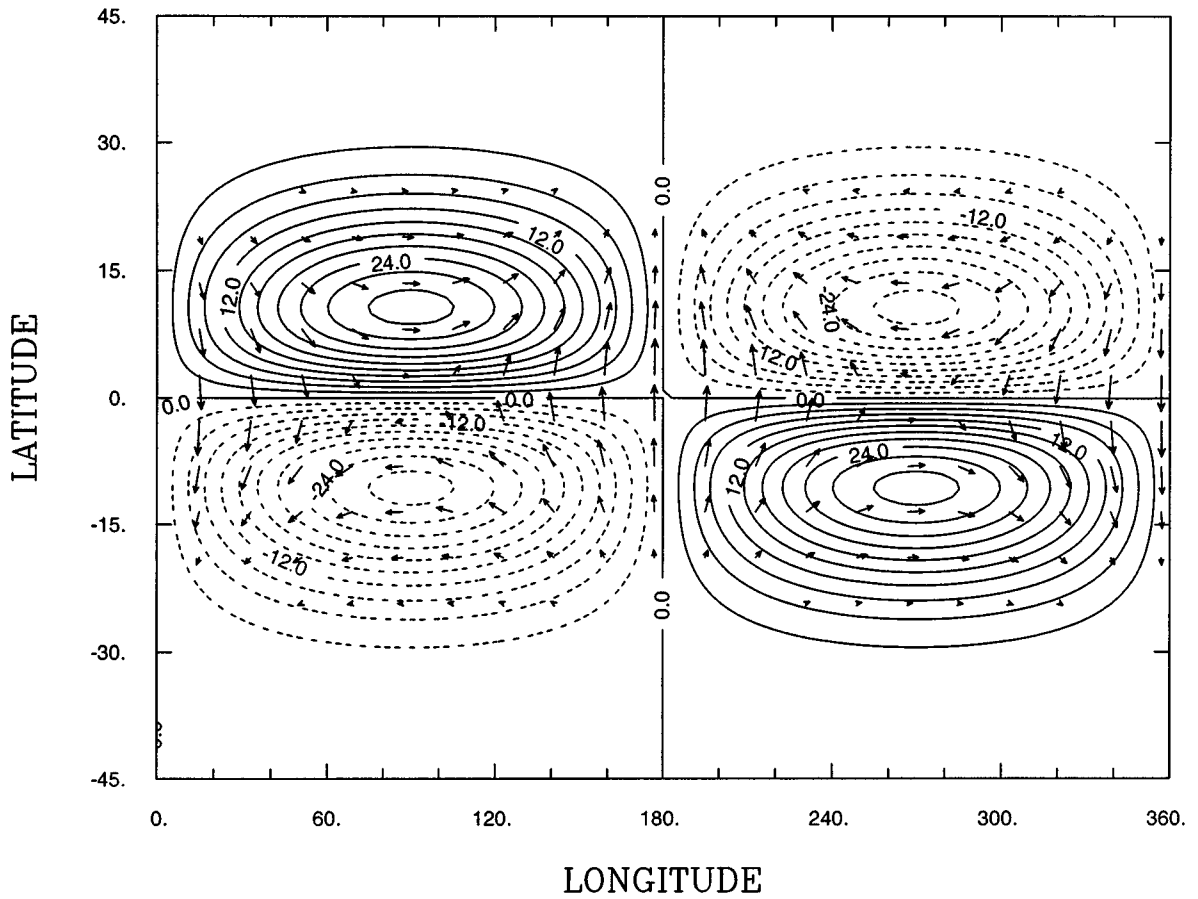
$$m \rightarrow \pm\infty \quad \text{when } |\hat{c}| \rightarrow 0$$

that is, the vertical wavelength $L_z = 2\pi/m$ vanishes as $\hat{c} \rightarrow 0$

- **Wave absorption** occurs when $|\hat{c}| \rightarrow 0$



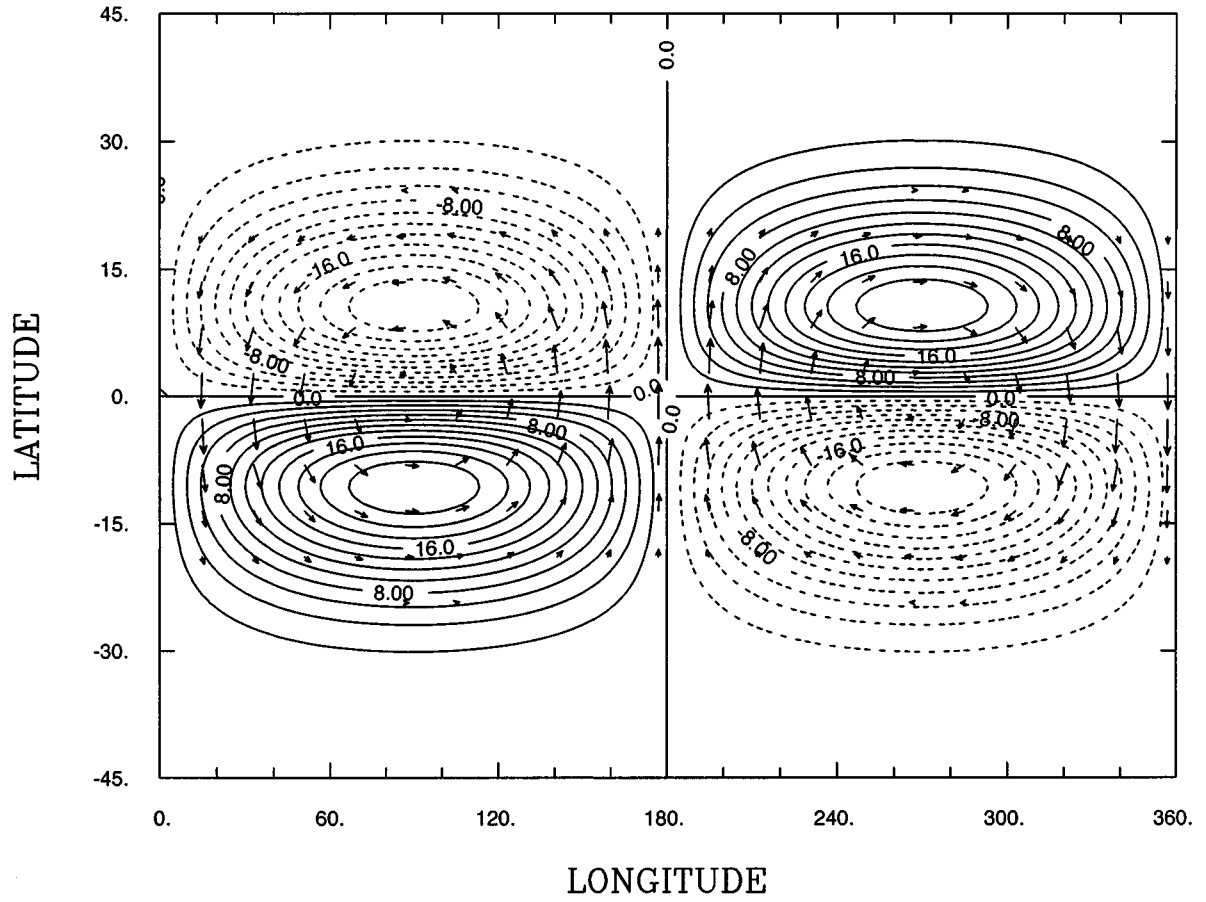
Phi $k = 1$, $Lz = 20$. km, $n = 0$, $f = 0.60$ cpd



CONTOUR FROM -30.000 TO 30.000 CONTOUR INTERVAL OF 3.0000 PT(3,3)=-0.54406E-02

0.100E+01
MAXIMUM VECTOR

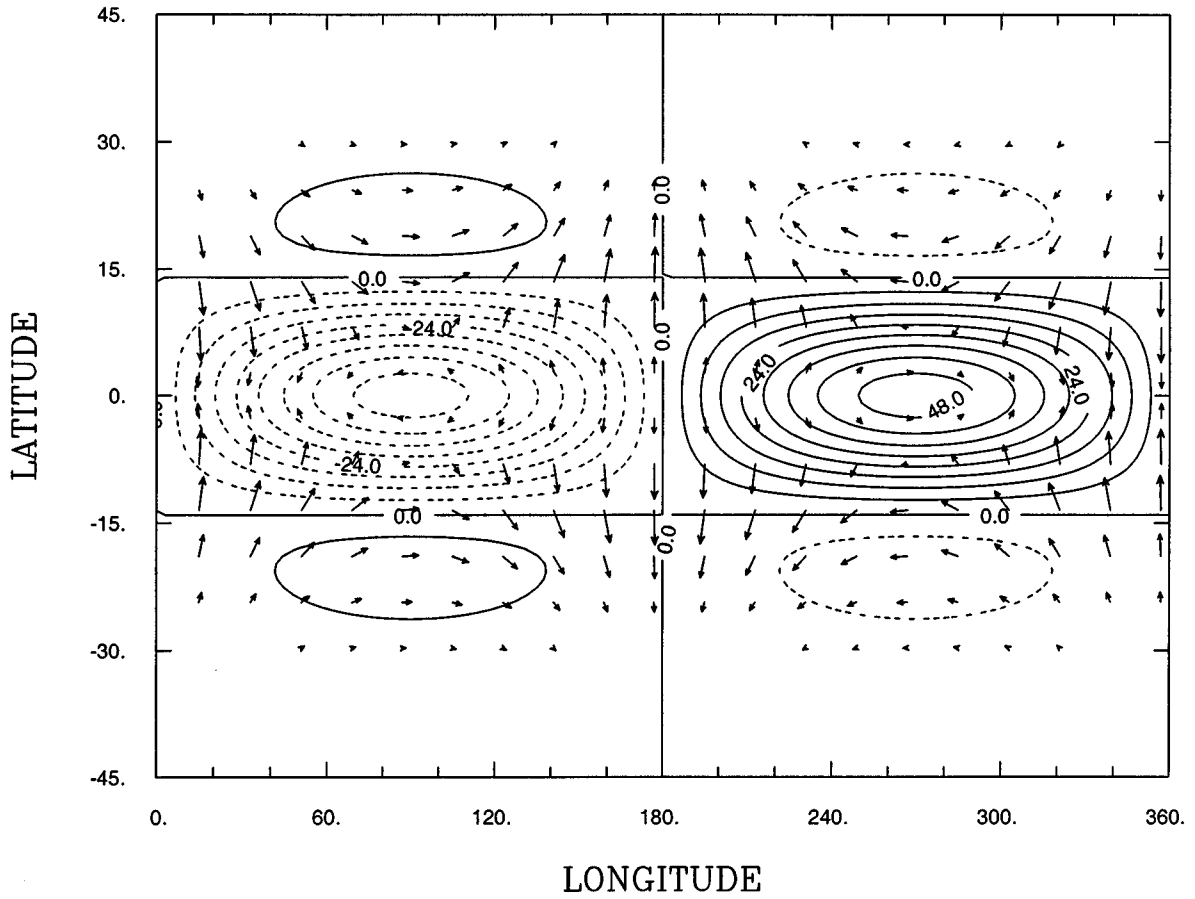
Phi $k = 1$, $Lz = 20$. km, $n = 0$, $f = -0.46$ cpd



CONTOUR FROM -22.000 TO 22.000 CONTOUR INTERVAL OF 2.0000 PT(3,3)= 0.41907E-02

0.100E+01
→
MAXIMUM VECTOR

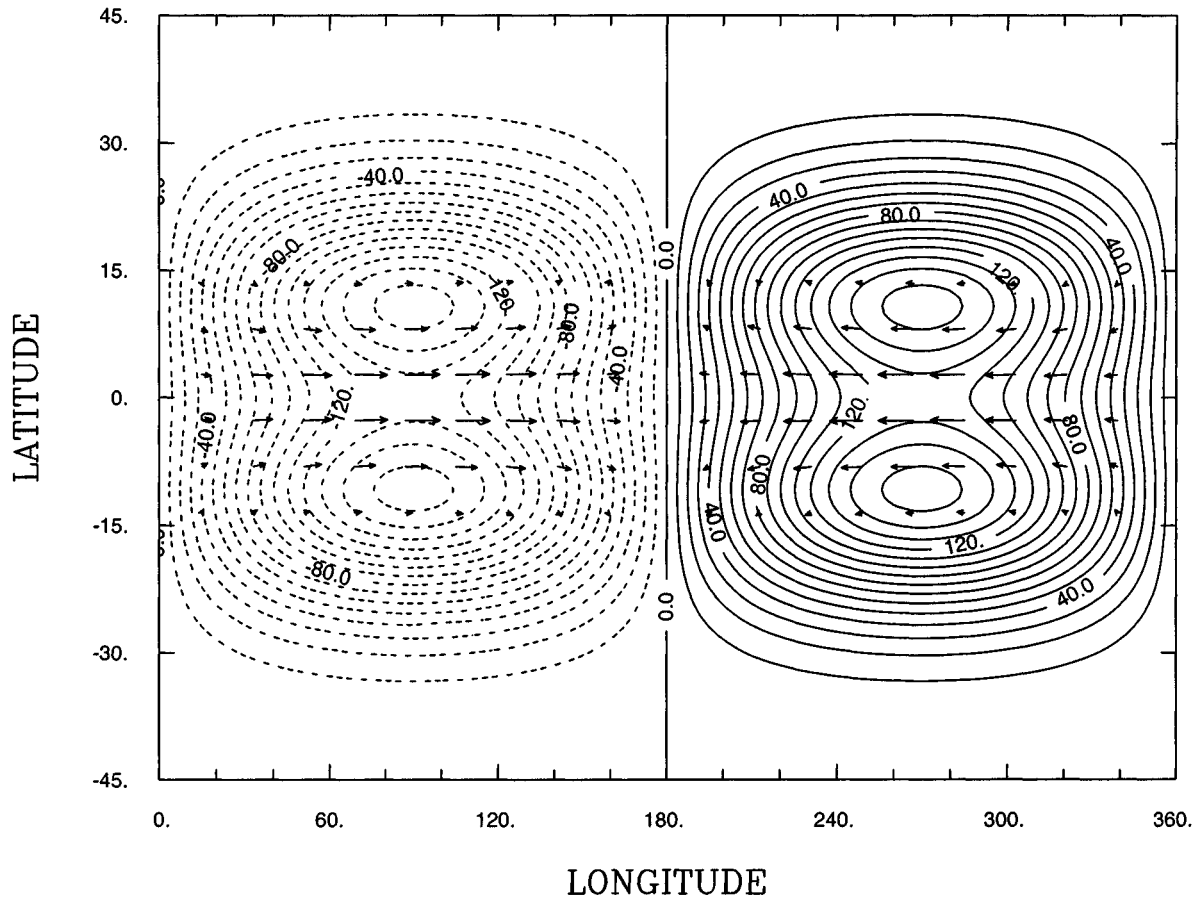
Phi $k = 1$, $Lz = 20$. km, $n = 1$, $f = 0.94$ cpd



CONTOUR FROM -48.000 TO 48.000 CONTOUR INTERVAL OF 6.0000 PT(3,3)= 0.11368E-01

0.606E+00
MAXIMUM VECTOR

Phi $k = 1$, $Lz = 20$. km, $n = 1$, $f = -0.04$ cpd



CONTOUR FROM -150.00 TO 150.00 CONTOUR INTERVAL OF 10.000 PT(3,3)=-0.59315E-01

0.604E+01
→
MAXIMUM VECTOR

Small-scale gravity waves

- Spatial and temporal scales are small enough that Coriolis force is not important
- Restoring force is gravity, acting through convergence/divergence
- We can use the equation derived earlier, this time ignoring the terms related to the Earth's rotation:

$$\left[\frac{d^2}{dy^2} + \left(\frac{m^2 \omega^2}{N^2} - k^2 \right) \right] \hat{v} = 0$$

- Since the coefficient is now constant, we can assume that

$$\hat{v} \propto \exp(i l y)$$

which yields the dispersion relation

$$\omega = \pm \frac{N}{|m|} (k^2 + l^2)^{1/2}$$

- This has the same form as the dispersion relation for inertia-gravity waves discussed earlier,

$$\omega = \pm \frac{N}{|m|} \left[k^2 + (2n + 1) \frac{\beta m}{N} \right]^{1/2}$$

where $(2n + 1)\beta m/N$ plays the role of a meridional wavenumber

- The two dispersion relations are identical in the large- k limit,

$$\omega = \pm \frac{Nk}{|m|}$$

- Small-scale gravity waves are ubiquitous in the Earth's atmosphere
 - they play a central role in extratropical dynamics
 - they may also play a leading role in the Tropics

Phase and Group Velocity

- The phase speed of a wave is given by $c = \omega/k$
- This is the speed at which crests and troughs of individual frequency components move
- In general, $c = c(k)$, a function of wavenumber
- An initial wave disturbance of arbitrary shape, or **wave packet**, can be expressed as a superposition of frequency and wavenumber components

$$\psi(x, t) = \sum A_{k, \omega} \exp i(kx - \omega t)$$

- The subsequent development of the wave packet does not, in general, preserve the initial shape since different components propagate at different rates
- Therefore, c is not the velocity at which wave energy propagates; i.e., it is not the velocity of the wave packet
- Consider the following simple example:

$$\psi(x, t) = \text{Re} \left\{ e^{i[(k+\Delta k)x - (\omega+\Delta\omega)t]} + e^{i[(k-\Delta k)x - (\omega-\Delta\omega)t]} \right\}$$

that is, a combination of two waves of slightly different k, ω

- This can be written as

$$\psi(x, t) = \text{Re} \left\{ e^{i(kx - \omega t)} \cdot \left[e^{i(\Delta kx - \Delta \omega t)} + e^{-i(\Delta kx - \Delta \omega t)} \right] \right\}$$

that is,

$$\psi(x, t) = 2 \cos(kx - \omega t) \cos(\Delta kx - \Delta \omega t)$$

or

$$\psi(x, t) = 2 \cos(kx - \omega t) \cos(\Delta k(x - c_g t))$$

where

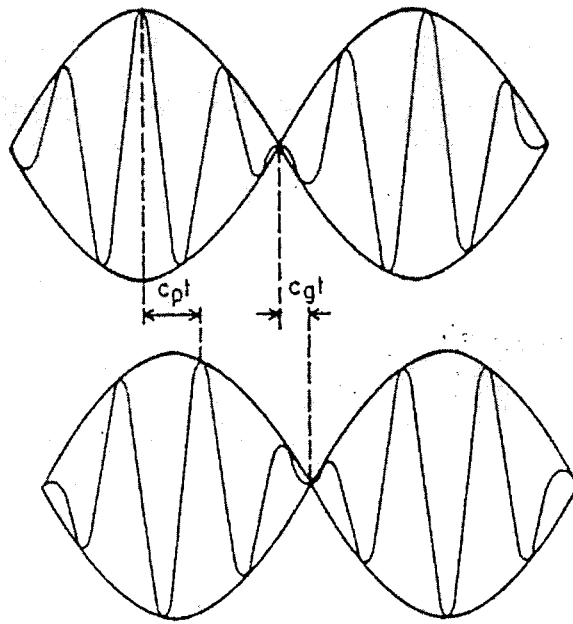
$$c_g = \frac{\Delta \omega}{\Delta k} \rightarrow \frac{\partial \omega}{\partial k}$$

is the **group velocity**

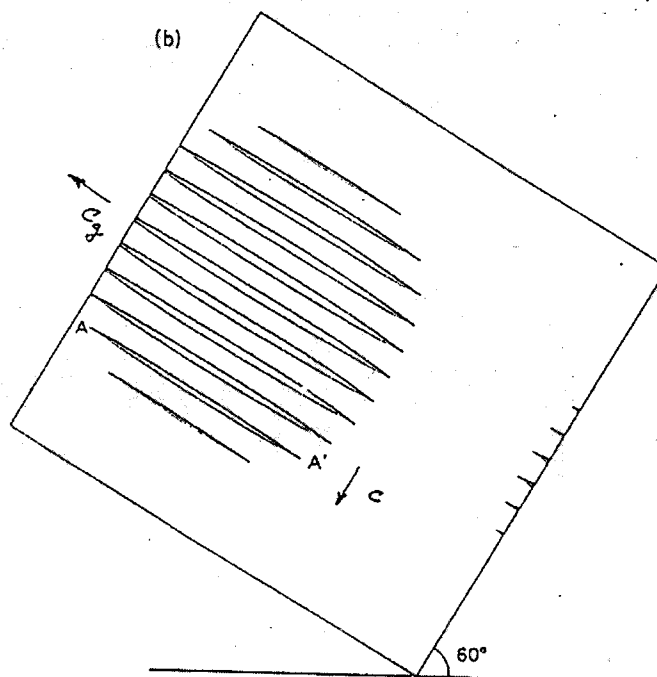
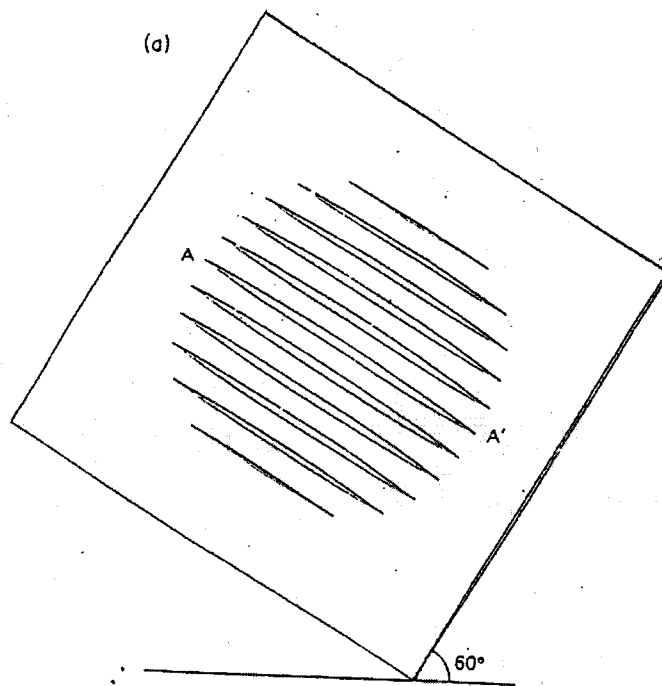
- Waves for which $c \neq c(k)$ are called nondispersive. In this case $\omega = kc$, $c_g = \partial \omega / \partial k = c$, and the wave packet retains its initial shape
- Otherwise, the envelopes of waves with different k travel at different rates, and the waves disperse as they propagate away from the source
- The group velocity result can be generalized to more than one dimension, so in general

$$c_g = \frac{\partial \omega}{\partial \mathbf{k}}$$

Dispersion



A superposition of two sinusoidal traveling waves, illustrating the difference between the speed c_p of the wave crests and the speed c_g of the envelope of the waves, i.e., of the regions of large amplitude. The group velocity c_g equals $d\omega/dk$



(a) The initial configuration of a group of internal waves with wave crests at 60° to the vertical. Contours are of pressure perturbation, where this is equal to $+0.5$ times the maximum value. (b) The configuration four periods later, the group having moved parallel to the crests and upward, while the individual crest AA' has moved four wavelengths downward and to the left.

Horizontal Group Velocity: Trapping

- The solution to the equation

$$\left[\frac{d^2}{dy^2} + \left(\frac{m^2 \omega^2}{N^2} - k^2 - \frac{k\beta}{\omega} \right) - \frac{\beta^2 m^2}{N^2} y^2 \right] \hat{v} = 0$$

can be written as follows in the WKB approximation:

$$\hat{v} = \frac{1}{\sqrt{l}} \exp i \left[kx + \int l(y') dy' + mz - \omega t \right]$$

where

$$\begin{aligned} l^2(y) &= \frac{m^2 \omega^2}{N^2} - k^2 - \frac{k\beta}{\omega} - \frac{\beta^2 m^2}{N^2} y^2 \\ &= \frac{\beta^2 m^2}{N^2} (y_c^2 - y^2) \end{aligned}$$

and

$$y_c^2 = \frac{\omega^2}{\beta^2} - \frac{k^2 N^2}{\beta^2 m^2} - \frac{k N^2}{\beta m^2 \omega}$$

- The solution is wavelike ($l^2 > 0$) as long as y is less than the “critical latitude” y_c
- This leads to wave trapping in $-y_c < y < y_c$

- The horizontal components of group velocity are

$$c_{gx} = \frac{\partial \omega}{\partial k} = \frac{2k + \beta \omega}{2\omega m^2 / N^2 + \beta k / \omega^2}$$

$$c_{gy} = \frac{\partial \omega}{\partial l} = \frac{2l}{2\omega m^2 / N^2 + \beta k / \omega^2}$$

- Then, the ray path in the x-y plane is defined by

$$\frac{dy}{dx} = \frac{c_{gy}}{c_{gx}} = \frac{l}{k + \beta / 2\omega}$$

$$\frac{d(y/y_c)}{1 - (y/y_c)^2} = \frac{\beta m / N}{k + \beta / 2\omega} \cdot dx$$

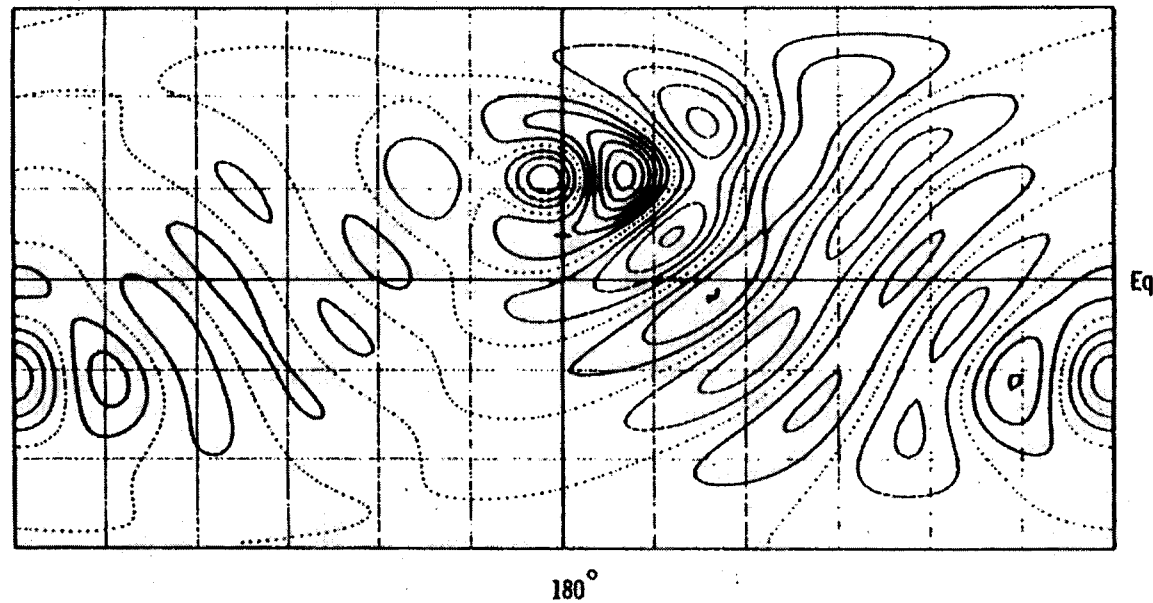
or

$$d[\sin^{-1}(y/y_c)] = \frac{\beta m / N}{k + \beta / 2\omega} \cdot dx$$

- Upon integration, this gives the ray path

$$y = y_c \sin \left(\frac{\beta m / N}{k + \beta / 2\omega} \cdot x \right)$$

- See Gill (1982) for a detailed discussion



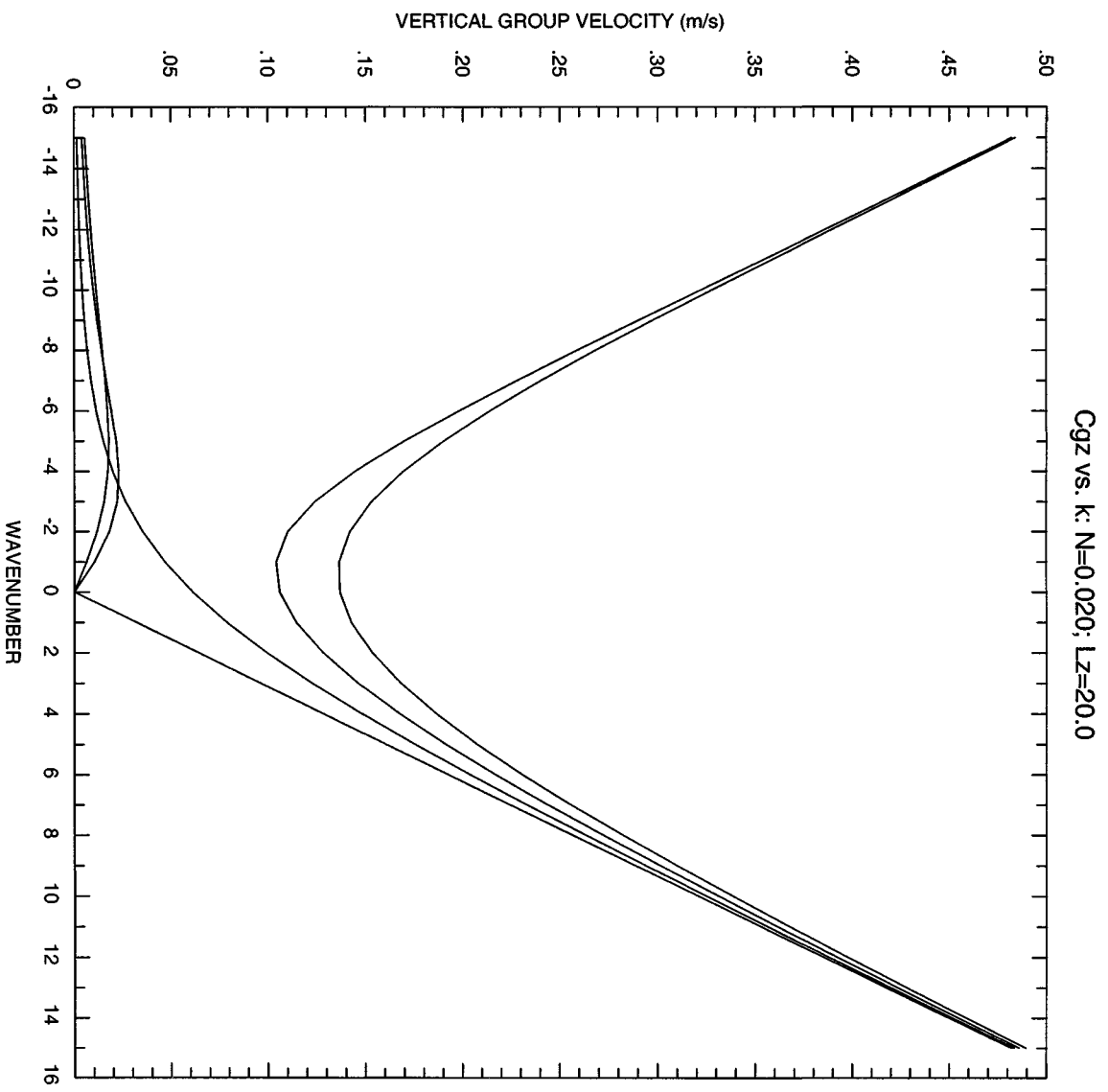
Planetary wave propagation on a sphere, as found in a numerical experiment of Grose and Hoskins (1979). Contours are of perturbation vorticity, and disturbances to a superrotation zonal flow (i.e., an eastward flow with uniform angular velocity about the earth's axis) are produced by a circular mountain centered at 30°N and 180° longitude, and with radius equal to 22.5° of latitude. Waves travel backward and forward across the equator along ray paths that are curved because of variation in the Coriolis parameter f with latitude. The equatorial trapping effect is evident. The amplitude of the wave decays with distance because of dissipative effects included in the model. [From Grose and Hoskins (1979, Fig. 3a).]

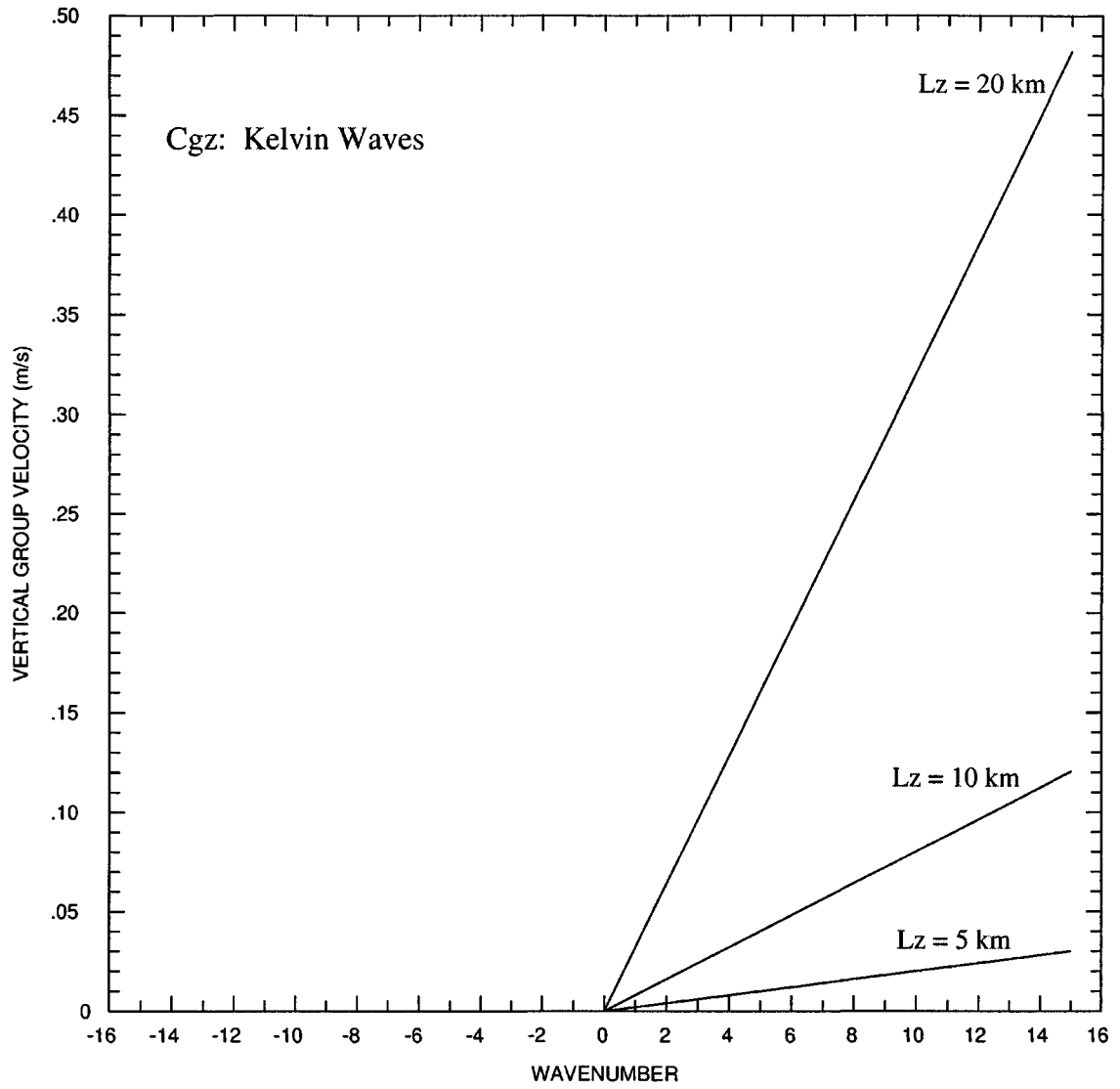
Vertical Group Velocity

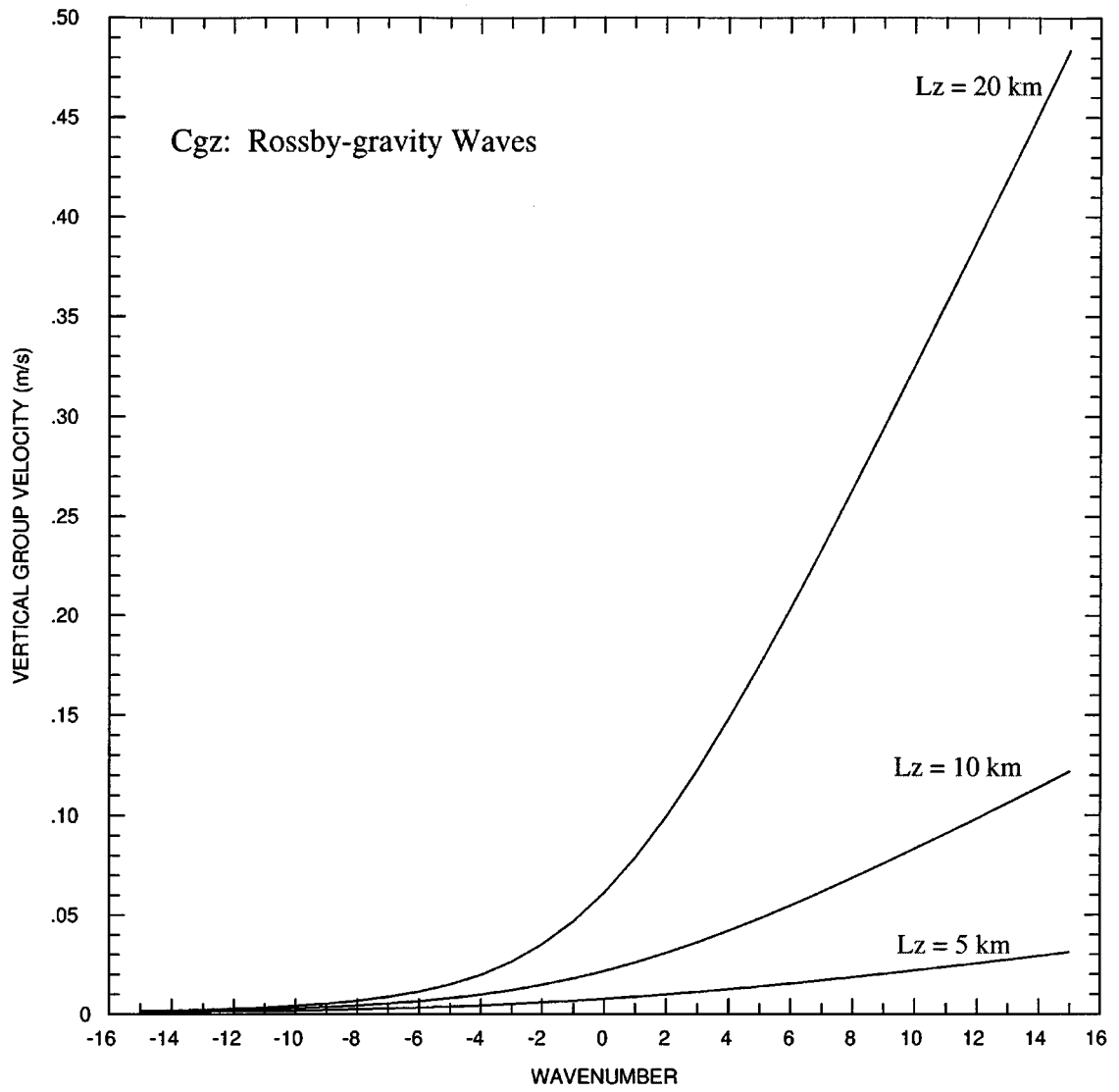
- Waves in the Tropics are excited by a variety of sources including
 - Direct absorption of solar radiation by atmospheric gases (ozone in the stratosphere, water vapor in the troposphere). Most important for the excitation of the thermal tides
 - Latent heat release by convection. This excites a broad spectrum of waves that are believed to be responsible for the driving of the QBO and SAO
- From the point of view of middle atmosphere dynamics, the most important waves are those that can propagate readily
- The effectiveness of vertical propagation depends on the waves' vertical group velocity,

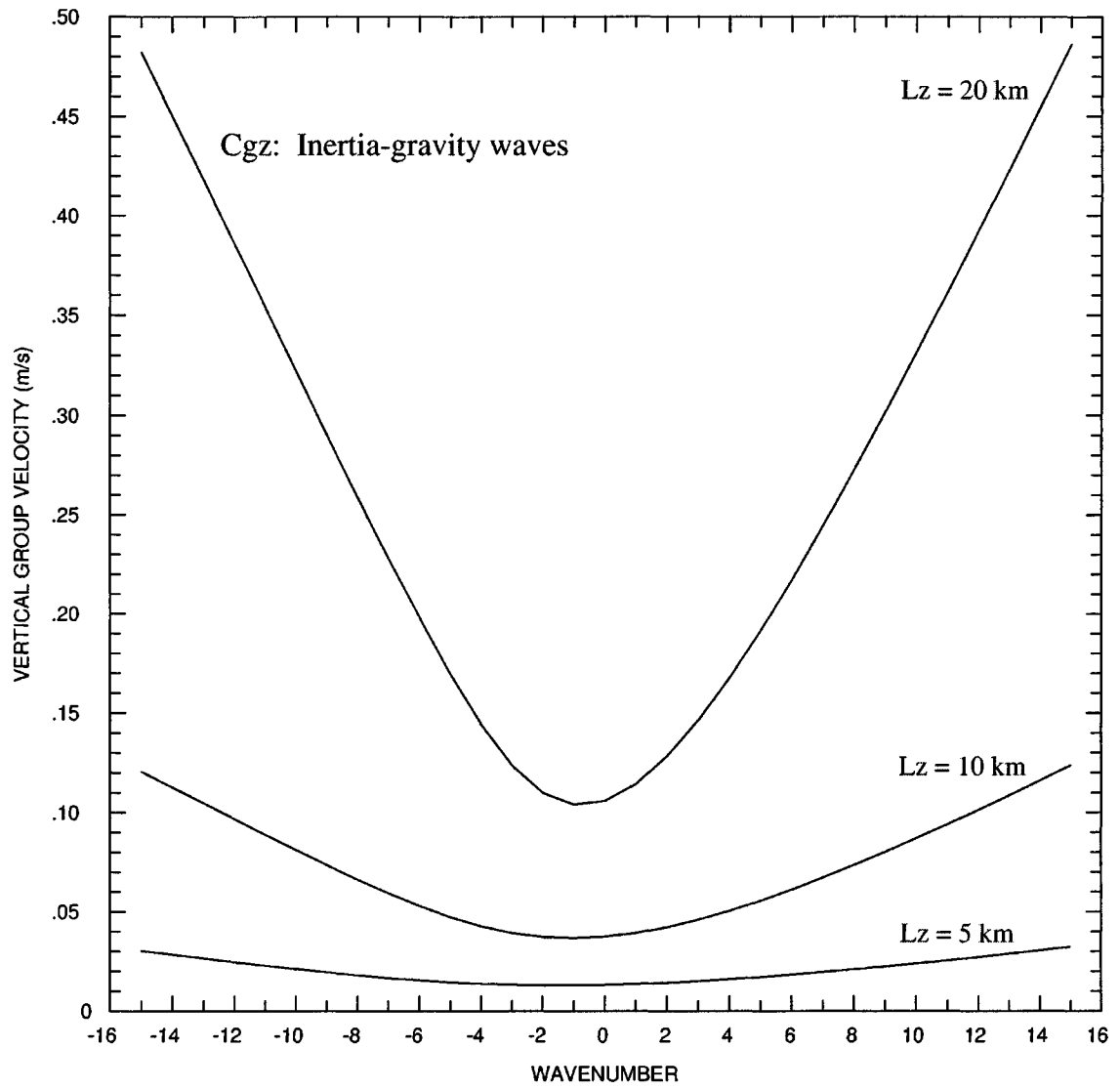
$$c_{gz} = \frac{\partial \omega}{\partial m}$$

- Waves with large c_{gz} are less subject to dissipation as they propagate vertically, so they can exert an influence at large altitudes
- Based upon these considerations, Kelvin and gravity waves should be of greatest importance for middle atmosphere dynamics
- For these waves, $c_{gz} \sim kN/m^2 \sim \omega^2/kN$









Vertical phase and group propagation

- Plane-parallel gravity waves have the dispersion relationship

$$\omega = -\frac{kN}{m}$$

- Eastward-propagating waves ($\omega > 0$) have $m < 0$
- Westward propagating waves ($\omega < 0$) have $m > 0$
- Note that Kelvin waves behave just like eastward-propagating gravity waves
- **Constant-phase lines in the $z - x$ plane** obey the relationship

$$kx + mz = C$$

where C is an arbitrary constant. Hence,

$$z = -\frac{k}{m} \cdot x \quad m < 0 \text{ for } \omega > 0 \text{ and } m > 0 \text{ for } \omega < 0$$

- Similarly, **constant phase lines in the $z - t$ plane** obey

$$mz - \omega t = C$$

whence

$$z = \frac{\omega}{m} \cdot t = -\left|\frac{\omega}{m}\right| \cdot t$$

(since $\omega m < 0$)

- The group velocities are

$$c_{gz} = \frac{kN}{m^2}$$

$$c_{gx} = -\frac{N}{m} \cdot t \quad m < 0 \text{ for } \omega > 0 \text{ and } m > 0 \text{ for } \omega < 0$$

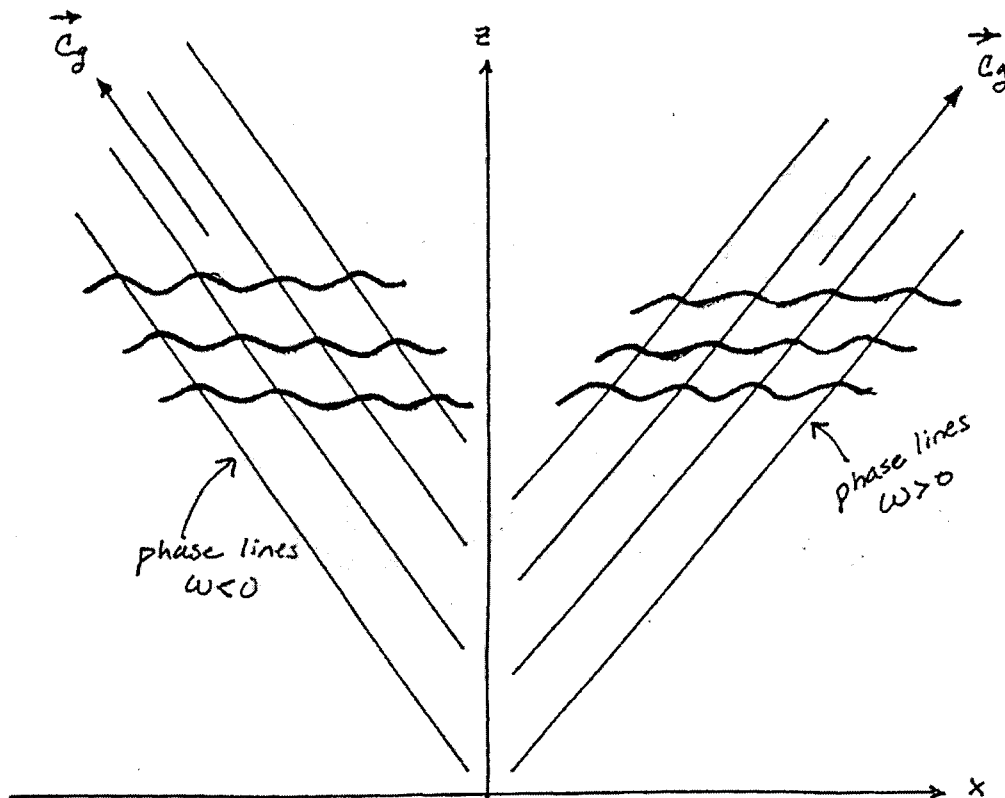
- Therefore, ray paths in the $x - z$ plane can be obtained from

$$\frac{dz}{dx} = \frac{c_{gz}}{c_{gx}} = -\frac{k}{m}$$

so that

$$z = -\frac{k}{m} \cdot x \quad m < 0 \text{ for } \omega > 0 \text{ and } m > 0 \text{ for } \omega < 0$$

- Comparing this with the behavior of phase lines in the $z - x$ plane, we see that the group velocity in the $z - x$ planes is parallel to lines of constant phase



$$\omega < 0 \quad m > 0$$

Constant phase

$$kx + mz = 0$$

$$\text{or, } z = -\frac{k}{m}x$$

Group Velocity

$$c_{gx} = -\frac{\omega}{k}, \quad c_{gz} = \frac{\omega}{m}$$

$$\omega > 0 \quad m < 0$$

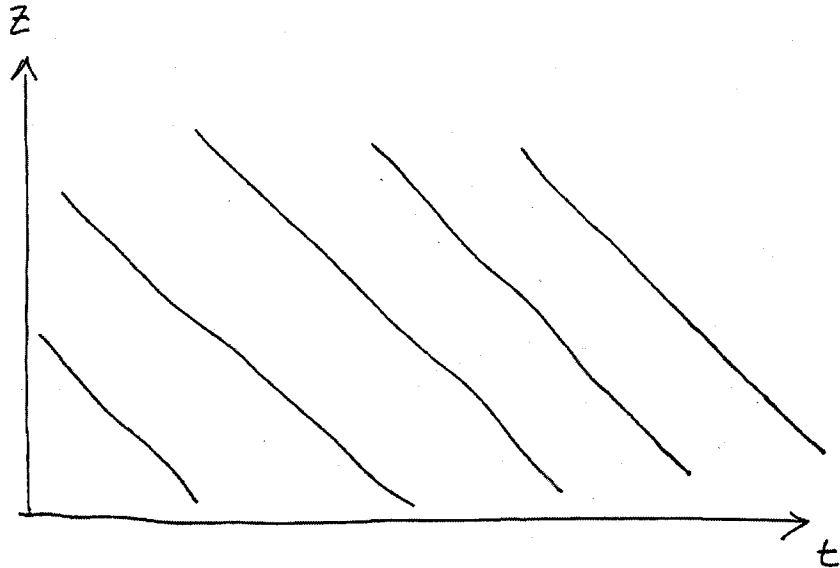
Constant phase

$$kx - |m|z = 0$$

$$\text{or, } z = \frac{k}{|m|}x$$

Group Velocity

$$c_{gx} = \frac{\omega}{k}, \quad c_{gz} = \frac{\omega}{|m|}$$



$$z = \frac{\omega}{m} \cdot t \quad \begin{array}{l} m < 0 \text{ for } \omega > 0 \\ m > 0 \text{ for } \omega < 0 \end{array}$$

⇒ Phase lines of upward-propagating waves slope downward with time:

$$z = - \left| \frac{\omega}{m} \right| \cdot t$$

Observations of Waves in the Tropics

- Large-scale waves are observable by conventional networks (radiosondes, rocketsondes) or by satellites (LIMS, UARS, etc)
- Large-scale waves in the Tropics were documented earliest and more thoroughly because
 - Generally occur at lower frequencies so sampling is easier
 - Have larger amplitudes at lower levels (lower, middle stratosphere)
 - Are detectable without aliasing by satellite platforms (these typically resolve up to 6 zonal wavenumbers and diurnal or longer periods)
- Smaller scale (and higher frequency) waves are harder to document, especially on a global basis
 - Often small amplitude at lower levels
 - Aliased in satellite observations
 - Detectable by lidar/radar/sonde observations, but coverage is limited
- Nevertheless, small scale and higher frequency waves are likely quite important for driving the QBO and SAO

- The following figures show examples of wave observations in the Tropics. After the publication of Matsuno's (1966) and other theoretical works on tropical waves, the existence of **large-scale Kelvin and Rossby-gravity waves** was documented in several studies
- Wallace and Gutzwiller (1968)
 - used radiosonde measurements of u and T from several tropical stations (Balboa, Trinidad, Kwajalein)
 - established the presence of a large-scale oscillation, and related it to the Kelvin wave predicted by theory
 - wave period was ~ 15 days and zonal wavenumber was $k = 1 - 2$
 - vertical wavelength of 6-10 km and phase velocity of 20 m s^{-1}
- Yanai and Maruyama (1966)
 - used radiosonde wind from several tropical Pacific stations
 - found a westward-propagating wave in the lower stratosphere, in westerly background winds
 - wave was present to about 22 km, where the winds became easterly
 - $\tau \sim 5$ days, $k \sim 4 - 5$, $c \sim -23 \text{ m s}^{-1}$

- Other **large-scale waves** were detected in rocket-sonde and satellite observations
- Hirota (1978)
 - used rocketsonde data from Ascension Island, giving information on u, v, T through the lower mesosphere
 - wavelike signals in u, T were prominent, not so in v
 - identified the oscillation as a Kelvin wave
 - $L_z \simeq 15 - 20$ km, $c \simeq 55 - 70$ m s⁻¹
 - wave amplitude found to depend on the phase of the SAO
- Since the late 1970's observations from polar-orbiting, limb-scanning satellites have provided global, synoptic views of **large-scale waves of low to moderate frequency**
- Coy and Hitchman (1984)
 - used observations of T by the LIMS instrument on Nimbus-7
 - observed a $k = 2$, eastward-propagating wave, identifiable as a Kelvin wave
 - $\tau = 6$ days, $L_z = 15$ km, $c_{gz} = 2.8$ km day⁻¹
 - $c \simeq 40$ m s⁻¹

- Salby et al (1984)
 - LIMS T observations to about 65 km
 - found concentration of spectral variance in the Tropics, consistent with Kelvin wave structure
 - wave periods become shorter at higher altitudes
 - documented the presence of $k = 1, 2$ waves
 - fast waves in lower mesosphere, $c \simeq 120 \text{ m s}^{-1}$, $L_z = 40 \text{ km}$

- Canziani et al (1994)
 - polar-orbiting satellite T data from MLS instrument on UARS
 - clearly established the presence of Kelvin waves, $k = 1, 2$ throughout the stratosphere
 - phase velocities in the range $c \simeq 30 - 115 \text{ m s}^{-1}$

- **Intermediate-scale, inertia-gravity waves** have also been observed by a variety of techniques. Note, however, that these waves are not observable by satellite instruments because their wavelengths (too small) and/or frequencies (often too high) cannot be resolved given sampling patterns of polar-orbiting satellites

- Cadet and Teitelbaum (1979)
 - observations of u, v using radar-tacked balloons during GATE (GARP Tropical Atlantic Experiment)
 - identified an inertia-gravity wave, consistent with meridional index $n = 1$
 - westward-propagating, small vertical wavelength, $\tau \simeq 1.5$ days

- Tsuda (1994)
 - detected oscillations in radiosonde data from Indonesia
 - waves present up to 35 km
 - eastward-propagating, $c \simeq 12 \text{ m s}^{-1}$, small vertical wavelength ($< 3 \text{ km}$)

- Sato and Dunkerton (1997)
 - Singapore radiosonde data
 - identified several Kelvin and inertia-gravity wave modes
 - zonal wavelengths ranging from about 1000 to perhaps 10,000 km
 - both eastward- and westward-propagation

Characteristics of the Dominant Observed Planetary-Scale Waves in the Equatorial Lower Stratosphere

Theoretical description	Kelvin wave	Rossby-gravity wave
Discovered by	Wallace and Kousky (1968)	Yanai and Maruyama (1966)
Period (ground-based) $2\pi\omega^{-1}$	15 days	4-5 days
Zonal wave number $s = ka \cos \phi$	1-2	4
Vertical wavelength $2\pi m^{-1}$	6-10 km	4-8 km
Average phase speed relative to ground	+25 m s ⁻¹	-23 m s ⁻¹
Observed when mean zonal flow is	Easterly (max. ≈ -25 m s ⁻¹)	Westerly (max. $\approx +7$ m s ⁻¹)
Average phase speed relative to maximum zonal flow	+50 m s ⁻¹	-30 m s ⁻¹
Approximate observed amplitudes		
u'	8 m s ⁻¹	2-3 m s ⁻¹
v'	0	2-3 m s ⁻¹
T'	2-3 K	1 K
Approximate inferred amplitudes		
Φ'/g	30 m	4 m
w'	1.5×10^{-3} m s ⁻¹	1.5×10^{-3} m s ⁻¹
Approximate meridional scales $\left(\frac{2N}{\beta m }\right)^{1/2}$	1300-1700 km	1000-1500 km

WALLACE AND KOUSKY (1968)

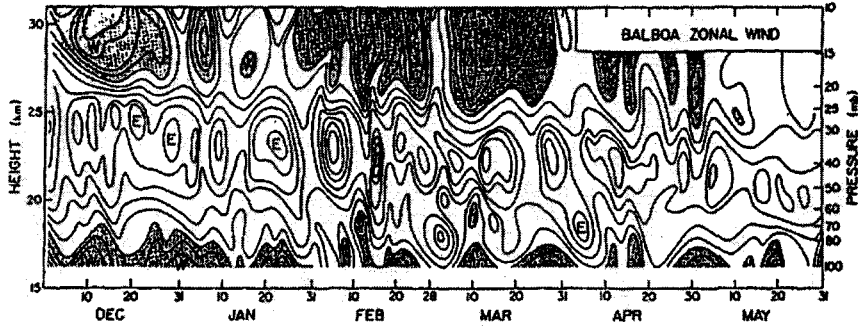


FIG. 2. Time-height section of zonal wind at Balboa. Isotachs are placed at intervals of 5 m sec^{-1} . Westerlies are shaded.

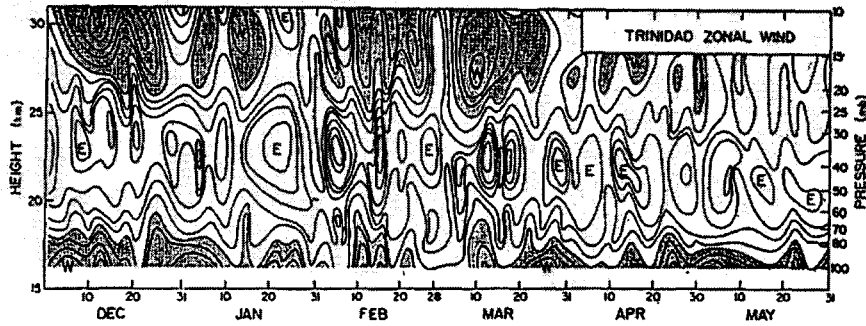


FIG. 6. Time-height section of zonal wind at Trinidad. Isotachs are placed at intervals of 5 m sec^{-1} . Westerlies are shaded.

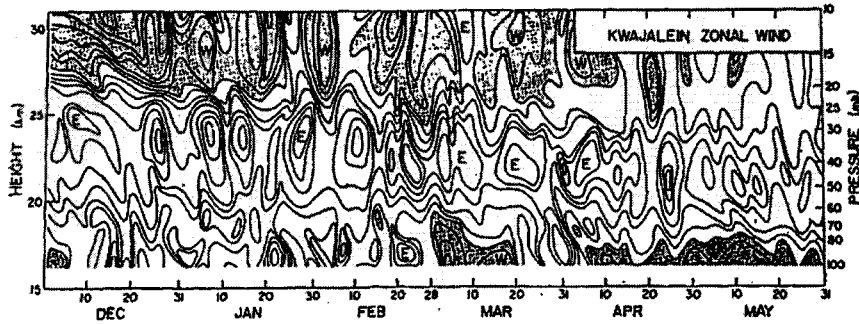


FIG. 4. Time-height section of zonal wind at Kwajalein. Isotachs are placed at intervals of 5 m sec^{-1} . Westerlies are shaded.

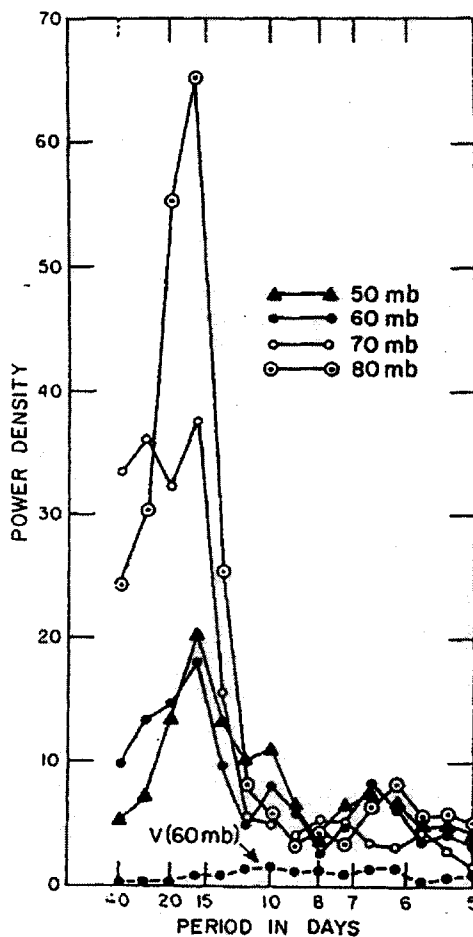


FIG. 8. Power spectra of zonal wind fluctuations at 80, 70, 60 and 50 mb shown together with the spectrum for the meridional wind fluctuations at 60 mb. Zonal wind data are prewhitened by means of a procedure described in the text.

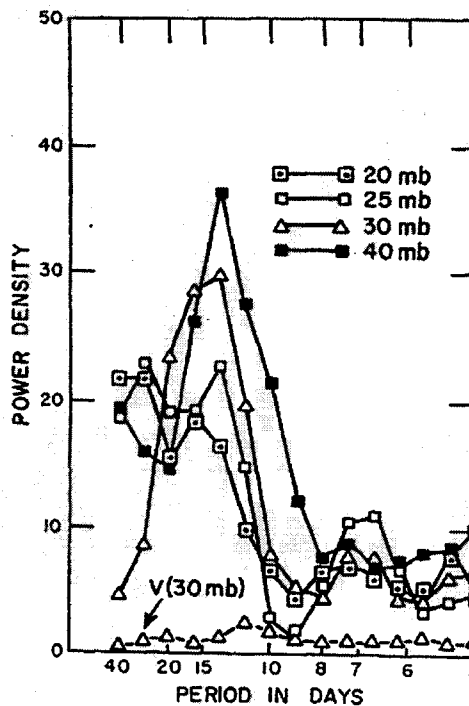


FIG. 9. Power spectra of zonal wind fluctuations at 40, 30, 25 and 20 mb shown together with the spectrum for the meridional wind fluctuations at 30 mb. Zonal wind data are prewhitened by means of a procedure described in the text.

YANAI AND MARUYAMA (1966)

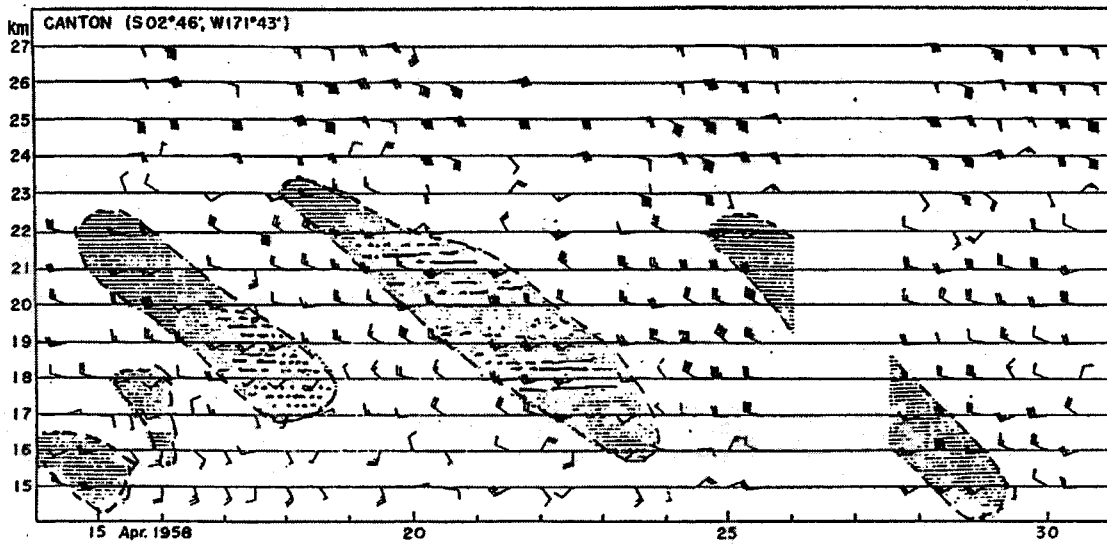


Fig. 3. Vertical time section of the lower stratospheric winds at Canton Island for 15-30 April 1958. Winds with southerly components are shaded.

YANAI AND MARUYAMA (1966)

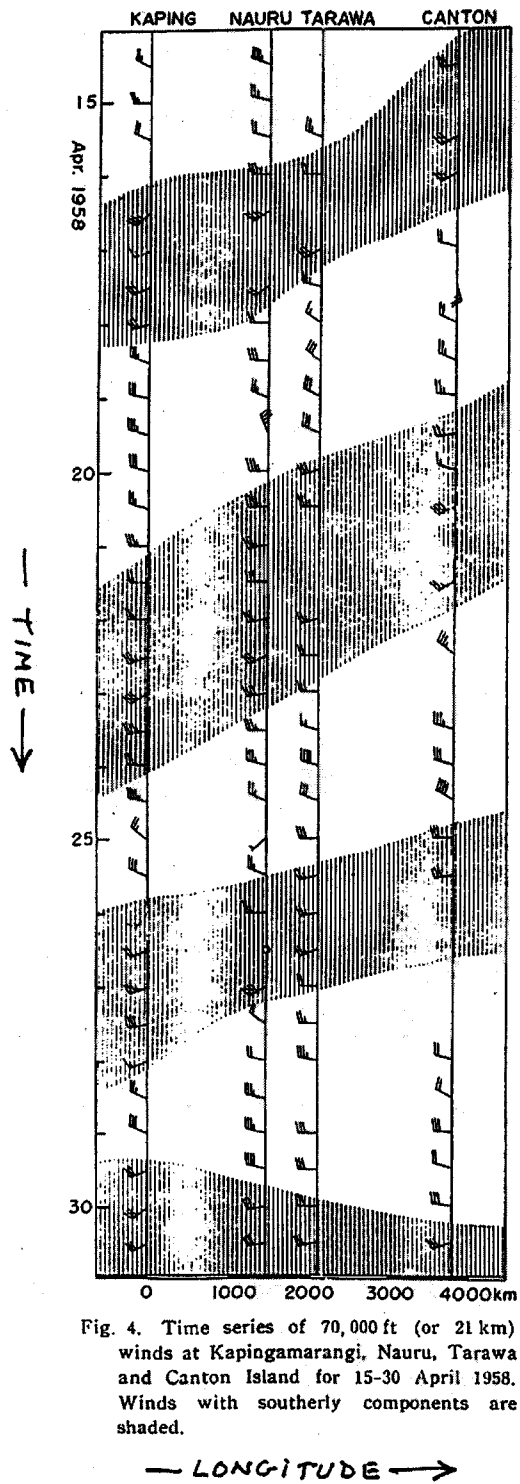


Fig. 4. Time series of 70,000 ft (or 21 km) winds at Kapingamarangi, Nauru, Tarawa and Canton Island for 15-30 April 1958. Winds with southerly components are shaded.

HIROTA (1978)

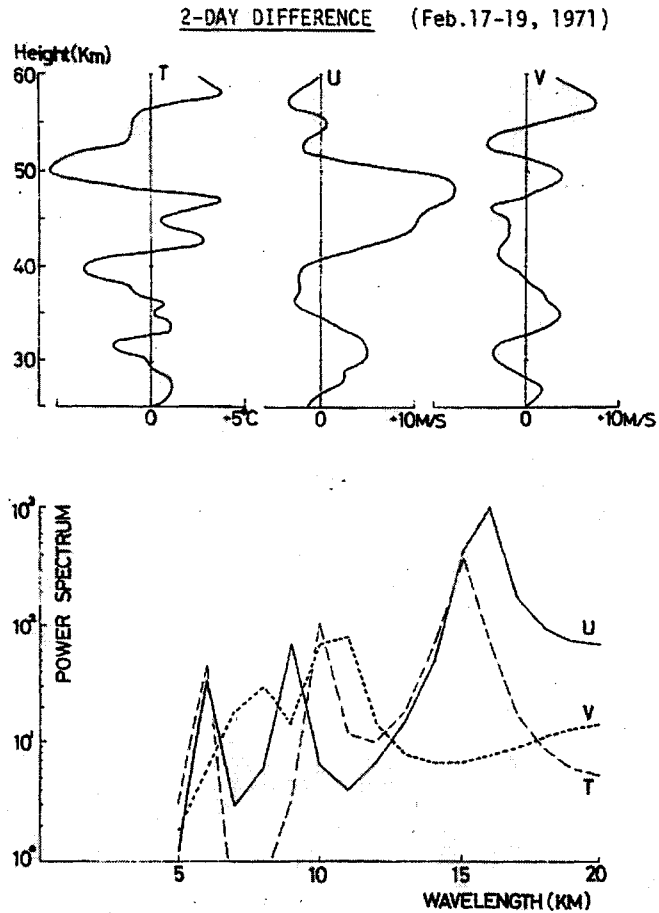


FIG. 3. An example of two-day difference of temperature (T) and zonal (U) and meridional (V) wind component (above) at Ascension Island for 17-19 February 1971. Units are $K \text{ day}^{-1}$ and $m \text{ s}^{-1} \text{ day}^{-1}$. Power spectra of each component are shown as a function of vertical wavelength (below). Units are $(K \text{ day}^{-1})^2 \text{ km}$ and $(m \text{ s}^{-1} \text{ day}^{-1})^2 \text{ km}$.

HIROTA (1978)

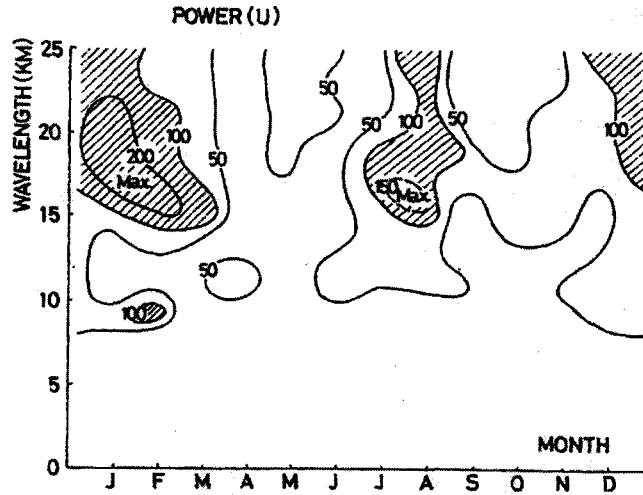
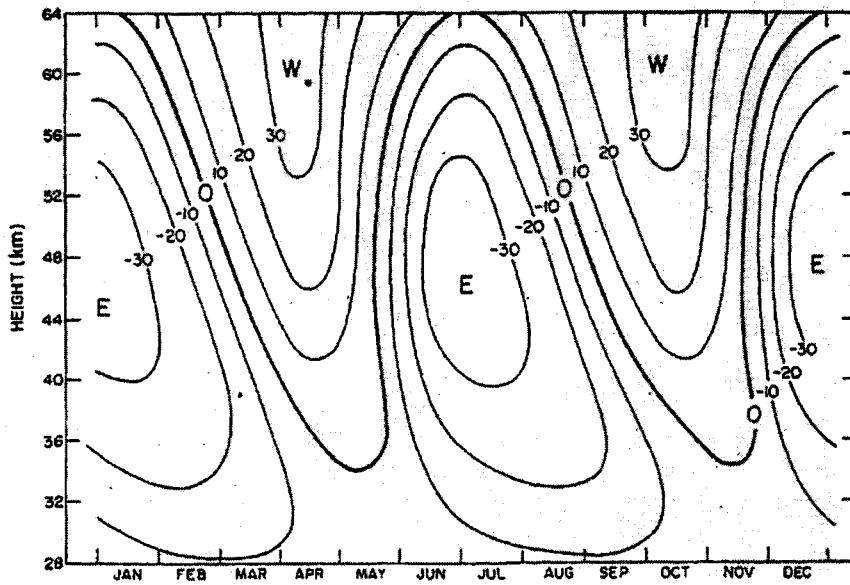


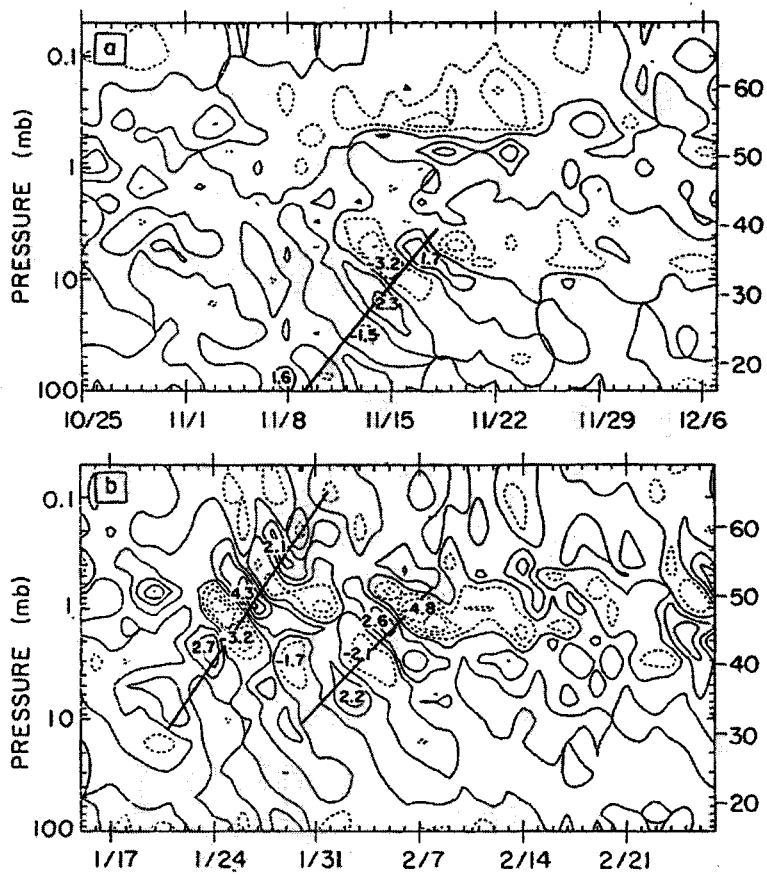
FIG. 6. Seasonal variation of power spectral density for the zonal wind component as a function of the vertical wavelength during the period of 1971 and 1972. Units are $(m\ s^{-1}\ day^{-1})^2\ km$.



Estimated variation of zonal wind (in $m\ sec^{-1}$) with month and altitude at the equator.

(Ascension I. rocketsondes)

Coy AND HITCHMAN (1984)



Equatorial time-height sections of LIMS zonal wave 2 temperature at 0° longitude for the periods (a) October 25 to December 7, 1978, and (b) January 15 to February 27, 1979. Contour interval of 1 K. [After Coy and Hitchman (1984).]

SALBY ET AL (1984)

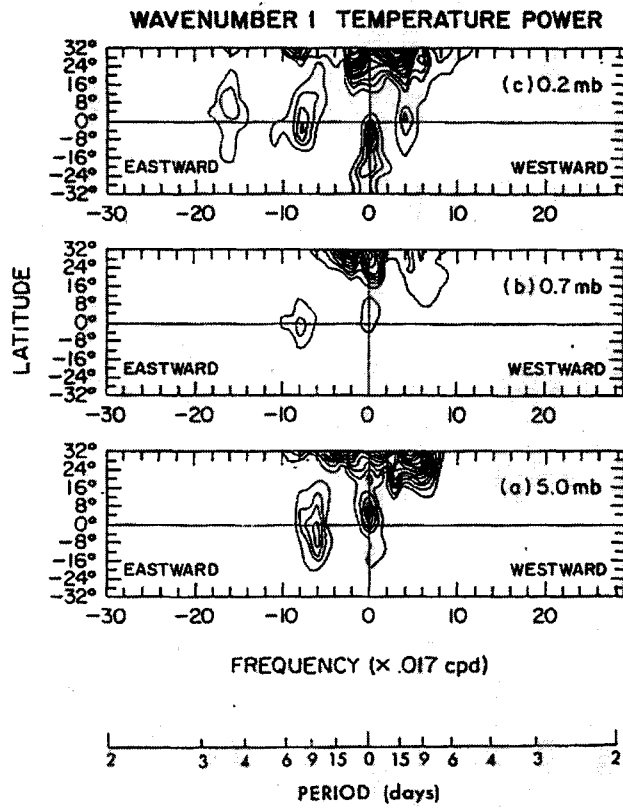


FIG. 6. Temperature power for wavenumber 1 as a function of frequency and latitude for the January-February sample period at (a) 5.0, mb contour increment = 0.02 K^2 , (b) 0.7 mb, contour increment = 0.10 K^2 , and (c) 0.2 mb, contour increment = 0.04 K^2 .

SALBY ET AL. (1984)

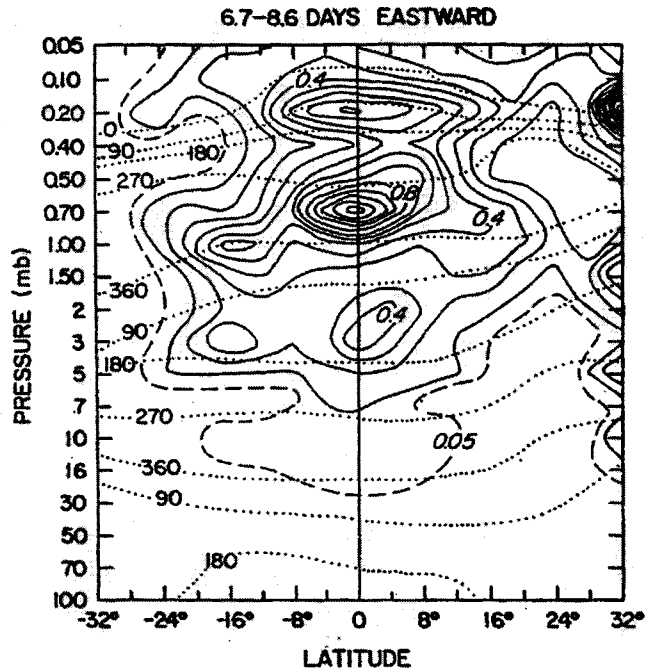


FIG. 7. Wavenumber 1 power (solid) and phase (dotted) structures, corresponding to the eastward spectra integrated between 6.7 and 8.6 days, ($54-69 \text{ m s}^{-1}$) as functions of latitude and pressure.

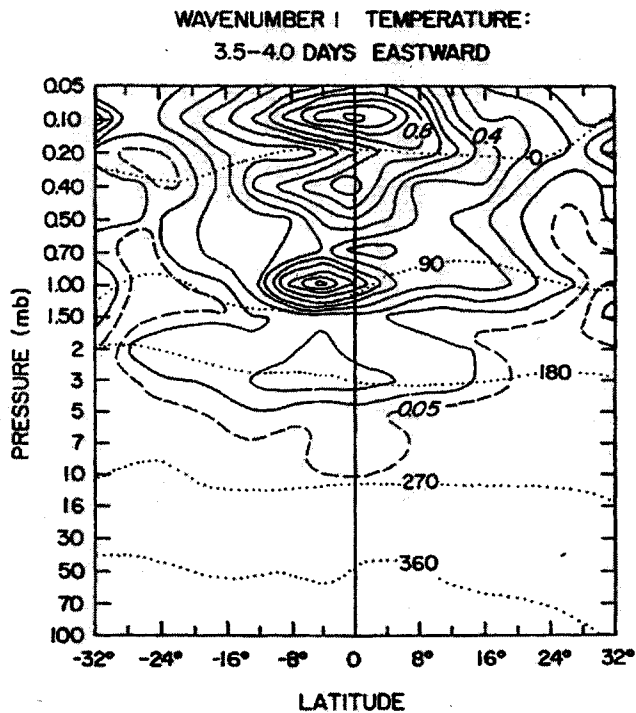


FIG. 8. As in Fig. 7, but for the faster wavenumber 1 feature, integrated between 3.5 and 4.0 days ($115-135 \text{ m s}^{-1}$). Contour increments as for Fig. 7.

SALBY ET AL (1984)

WAVENUMBER 2 TEMPERATURE:
6.0-7.5 DAYS EASTWARD

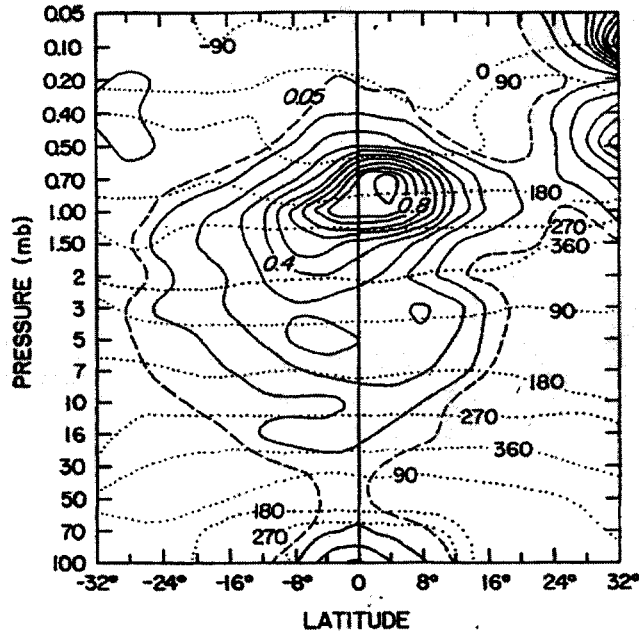


FIG. 12. Wavenumber 2 power (solid) and phase (dotted) structures, corresponding to eastward spectra integrated between 6.0 and 7.5 days ($31-39 \text{ m s}^{-1}$), as functions of latitude and pressure. Contour increments as for Fig. 7.

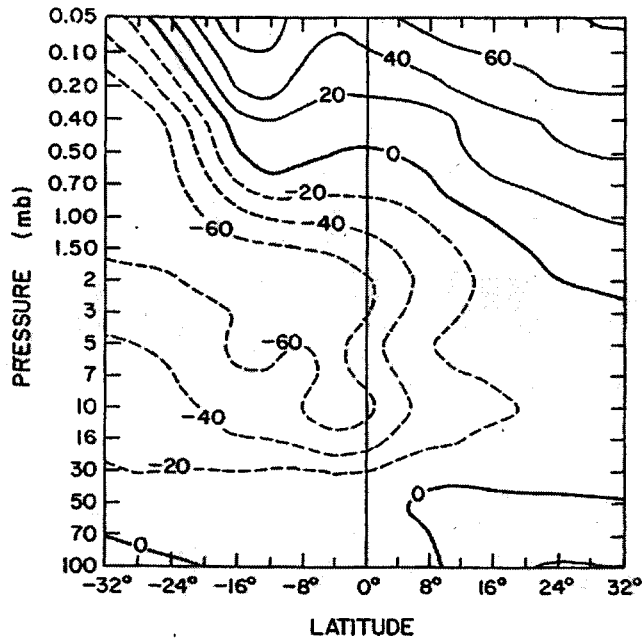


FIG. 18. Average zonal-mean wind speed (m s^{-1}) for 31 January-6 February 1979. Courtesy M. Hitchmann.

CANZIANI ET AL. (1994)

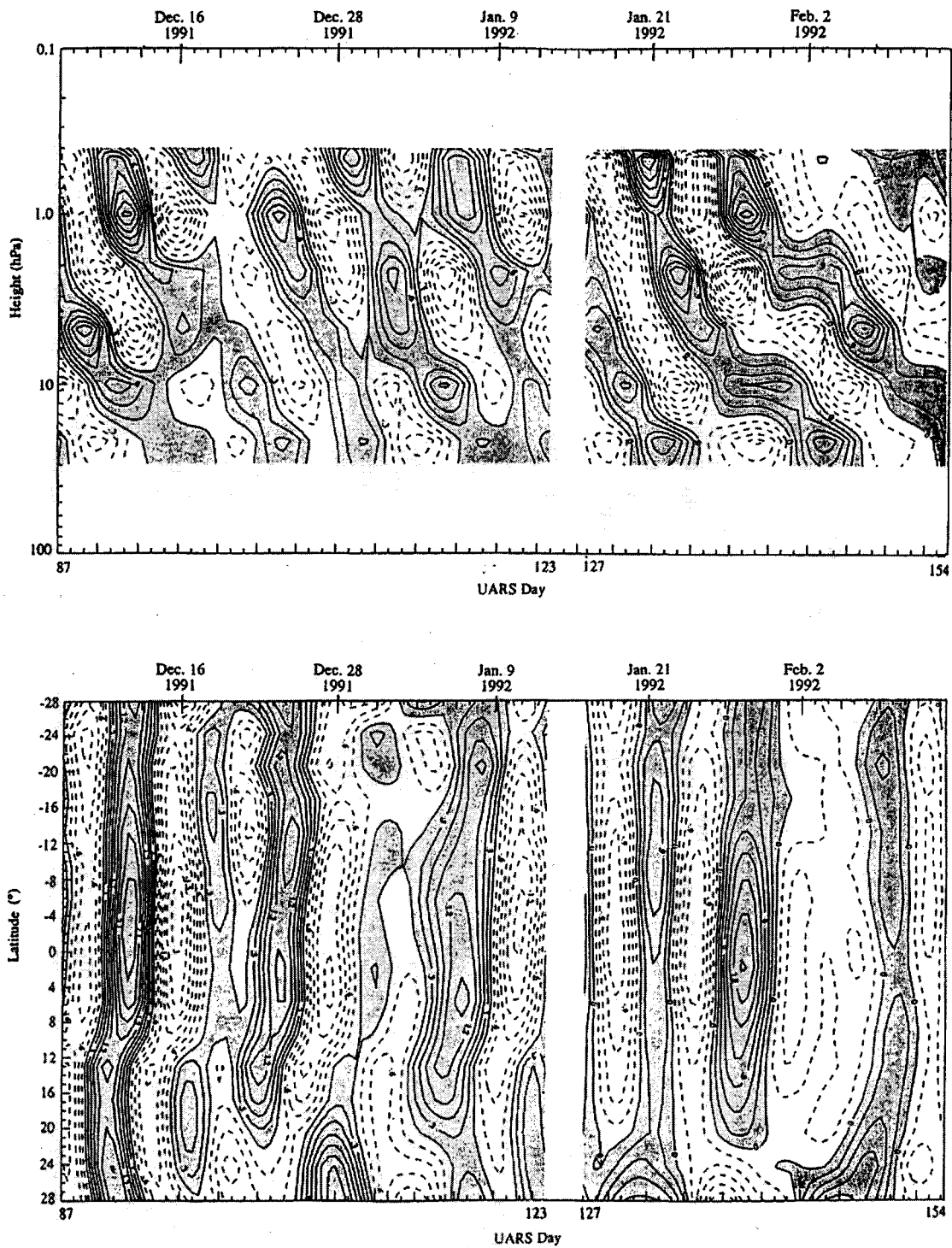


FIG. 3. (a) Time-height plot at the equator and (b) latitude-time plot at 1 hPa of temperature zonal wavenumber 1, bandpassed for periods between 5.5 and 20 days, during period 1, at 0° longitude. Positive values are highlighted in gray. (Contour interval is 0.3°C.)

CANZIANI ET AL (1994)

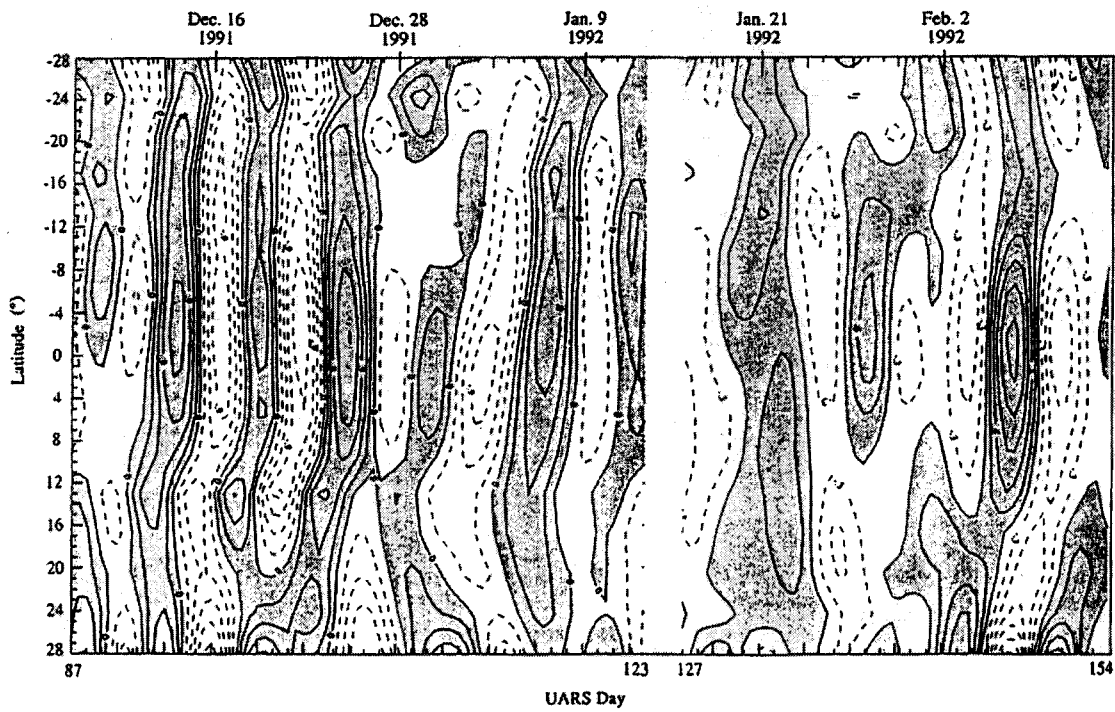
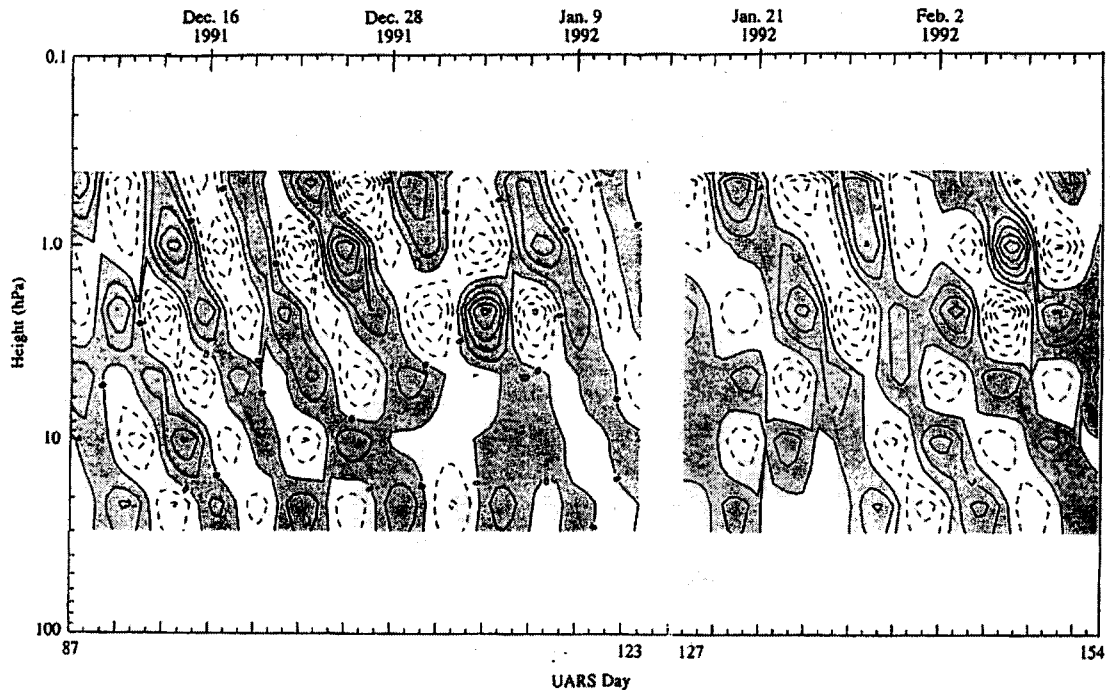


FIG. 4. Same as Fig. 3 but for zonal wavenumber 2 with periods between 2.5 and 4.5 days.

TABLE 1. Some properties of Kelvin waves detected in MLS temperature and ozone fields.

Sample period	Zonal wavenumber	Zonal phase speed (m s^{-1})	Observed period (days)	Intrinsic period (days) at various altitudes				Vertical wavelength (km)
				20 hPa	10 hPa	5 hPa	1 hPa	
I	1	57.9	8.0	6.0	6.6	6.5	5.6	20
I	1	115.8	4.0	3.4	3.6	3.6	3.3	44
I	2	38.6	6.0	4.0	4.5	4.5	3.6	14
I	2	57.9	4.0	3.0	3.3	3.3	2.8	20
II	1	66.2	7.0	7.0	6.3	5.8	5.9	20
II	1	102.9	4.5	4.5	4.2	4.0	4.1	30
II	2	29.0	8.0	8.0	6.4	5.4	5.5	14
II	2	57.9	4.0	4.0	3.6	3.2	3.3	20

CADET AND TEITELBAUM (1979)

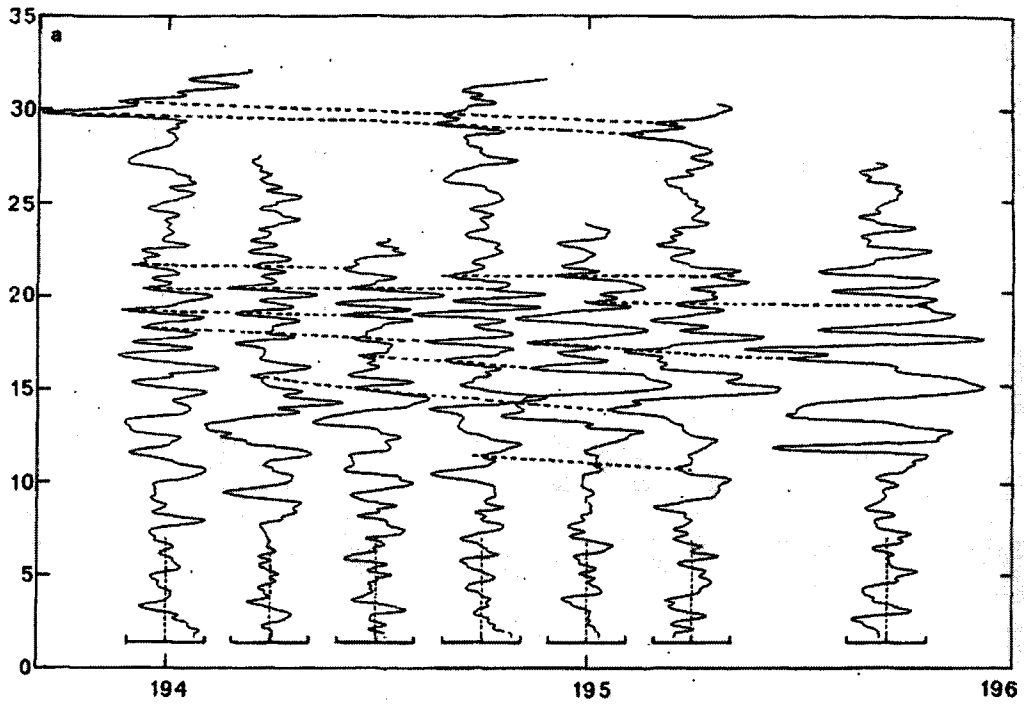
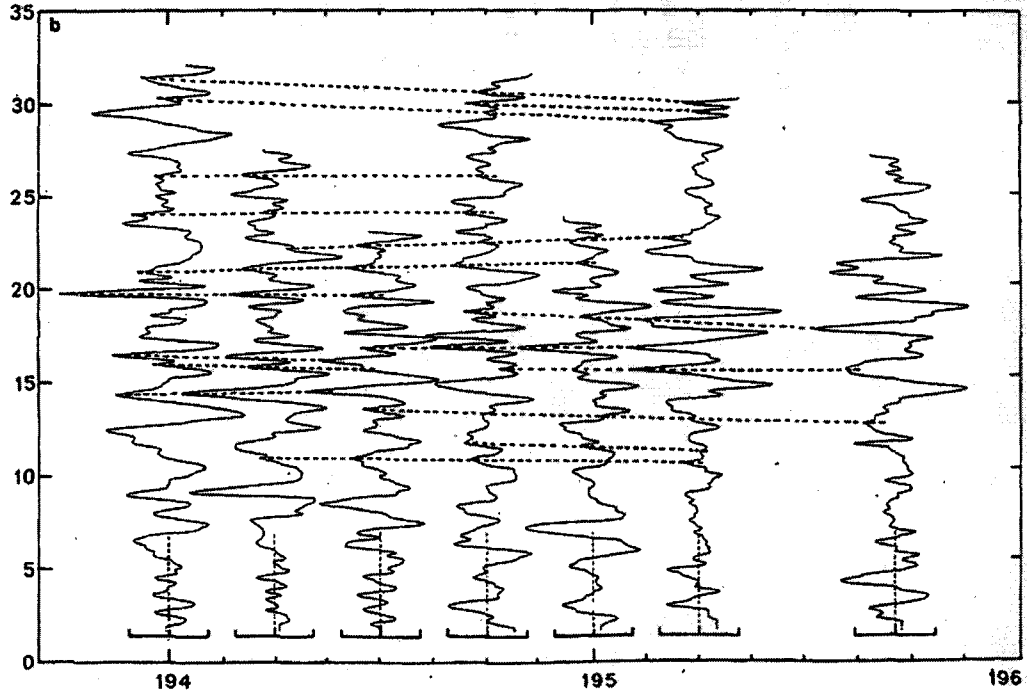


FIG. 8a. Sequence of vertical profiles of the u component in the vertical wavelength band 200-1500 m. Phase 1. The abscissa for each time is shifted so that the origin is indicated by vertical dashed lines. Time is in Julian Days.



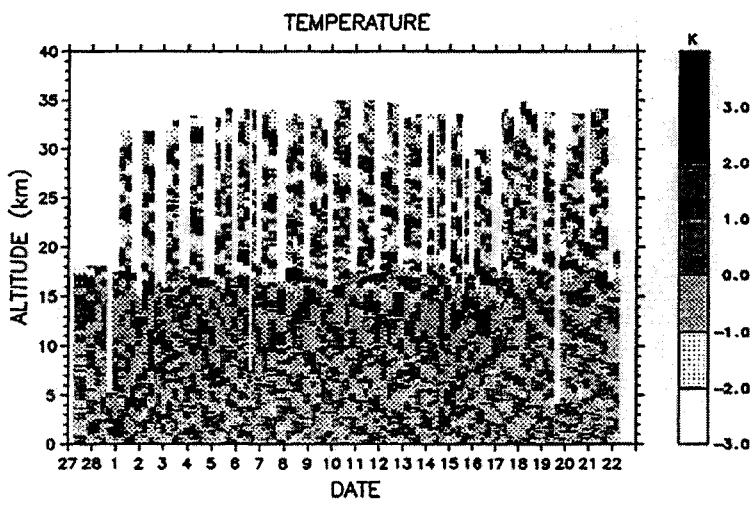
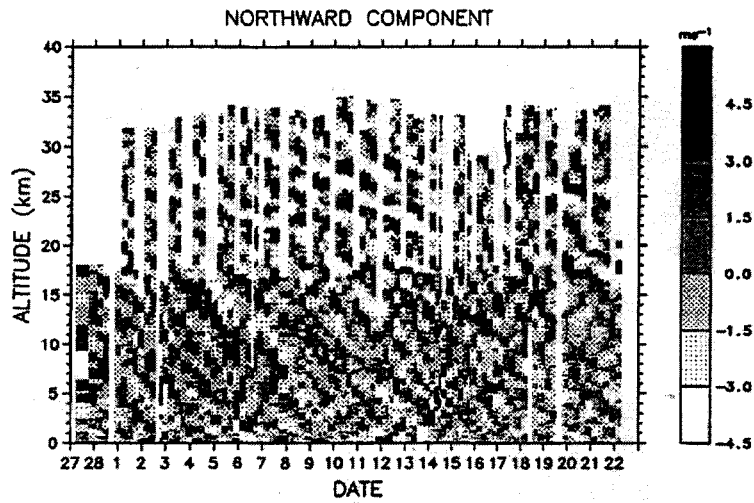
Sequence of vertical profiles of the v component in the vertical wavelength band 200-1500 m. Phase 1.

CADDET AND TEITELBAUM (1979)

TABLE 1. Characteristics of the waves deduced from the analysis of wind profiles.

Parameter	Value
Period	35 h
Zonal wavelength	2400 km
Horizontal phase speed (relative to the ground)	-20 m s^{-1}
Vertical wavelength (in a zero wind profile)	5 km
Vertical phase speed (in a zero wind profile)	-4 cm s^{-1}
Amplitudes	
zonal wind	3 m s^{-1}
meridional wind	2 m s^{-1}

TSUDA ET AL. (1994)



Contour plots of the (top) northward wind velocity and (bottom) temperature fluctuations.

SATO AND DUNKERTON (1997)

Table 1. Parameters of Possible Equatorial Waves for Observed 1–3 Day Components in Westerly Shear

Mode	c , m s^{-1}	λ_x , km	λ_z , km	y_0 , $\times 10^3$ km
$n = -1$ Kelvin waves	>6.7	>870	>2.0	>550
$n = 1$ eastward IGW	7.7–19.6	1000–2500	2.0–4.2	550–790
$n = 3$ eastward IGW	9.4	1200	2.0	550
$n = 1$ westward IGW	–25 to –31.8	3200–4100	5.7–6.7	920–1010

The zonal phase velocity, zonal wavelength, vertical wavelength, latitudinal scale factor are denoted by c , λ_x , λ_z , and y_0 , respectively. IGW, inertia-gravity waves.

Table 2. Same as Table 1 but for Easterly Shear

Mode	c , m s^{-1}	λ_x , km	λ_z , km	y_0 , $\times 10^3$ km
$n = -1$ Kelvin waves	>15	>1900	>2.7	>820
$n = 1$ eastward IGW	15–44.1	1900–5700	3.4–6.6	710–970
$n = 3$ eastward IGW	15–20.6	1900–2700	2.6–3.1	630–660
$n = 1$ westward IGW	–7.2 to –61.8	930–8000	2.0–9.3	550–1180
$n = 3$ westward IGW	–8.6 to –23.8	1100–3100	2.0–3.6	550–730
$n = 5$ westward IGW	–11.7 to –14.7	1500–1900	2.0–2.2	550–570

CONCLUSIONS

- Equatorial wave theory is able to define the characteristics of waves in the Tropics, at least under idealized conditions
- Theoretical results can be used to identify and interpret wave behavior in the real world
- Observations of tropical waves are abundant since the mid-1970's
- With satellite observations, the presence, morphology, and behavior of large-scale, low to moderate frequency waves is well documented
- Global forcing of the mean state due to large-scale waves can be estimated
- Smaller-scale, higher-frequency waves are more difficult to document because they are often aliased in satellite observations
- Nevertheless, observations of these waves (Kelvin, inertia-gravity) are now plentiful
- Observations of mesoscale ($L_x \sim 100$ km) gravity waves are also becoming common
- The challenge remains to determine the effect of the smaller-scale waves on the mean state of the Tropics

BIBLIOGRAPHY

- Baldwin, M.P., et al., 2001: The quasi-biennial oscillation. *Rev. Geophys.*, **39**, 179-229.
- Cadet, D. and H. Teitelbaum, 1979: Observational evidence of inertia-gravity waves in the tropical stratosphere. *J. Atmos. Sci.*, **36**, 892-907.
- Coy, L. and M. Hitchman, 1984: Kelvin wave packets and flow acceleration: A comparison of modeling and observations. *J. Atmos. Sci.*, **41**, 1875-1880.
- Gill, A.E., 1982: **Atmosphere-Ocean Dynamics**. Academic Press, London.
- Hirota, I., 1978: Equatorial waves in the upper stratosphere and mesosphere in relation to the semiannual oscillation of the zonal wind. *J. Atmos. Sci.*, **35**, 714-722.
- Hirota, I. and T. Niki, 1985: A statistical study of inertia-gravity waves in the middle atmosphere. *J. Meteor. Soc. Japan*, **63**, 2055-1066.
- Matsuno, T., 1966: Quasi-geostrophic motions in the equatorial area. *J. Meteor. Soc. Japan*, **44**, 25-42.
- Salby, M.L., D.L. Hartmann, P.L. Bailey, and J.C. Gille, 1984: Evidence for equatorial Kelvin modes in Nimbus-7 LIMS. *J. Atmos. Sci.*, **41**, 220-235.
- Sato, K. and T.J. Dunkerton, 1997: Estimates of momentum flux associated with equatorial Kelvin and gravity waves. *J. Geophys. Res.*, **102**, 26,247-26,261.
- Tsuda, T., Y. Maruyama, H. Wiryosumarto, Sri Woro B. Harijono, and S. Kato, 1994: Radiosonde observations of equatorial atmospheric dynamics over Indonesia. 2. Characteristics of gravity waves. *J. Geophys. Res.*, **99**, 10,507-10,516.
- Wallace, J.M. and V.E. Kousky, 1968: Observational evidence of Kelvin waves in the tropical stratosphere. *J. Atmos. Sci.*, **25**, 900-907.
- Yanai, M. and T. Maruyama, 1966: Stratospheric wave disturbances propagating over the equatorial Pacific. *J. Meteor. Soc. Japan*, **44**, 291-294.